NeuroImage 62 (2012) 250–265

Contents lists available at SciVerse ScienceDirect

NeuroImage

journal homepage: www.elsevier.com/locate/ynimg

Electrophysiological and functional connectivity of the human supplementary motor area

Shalini Narayana [a,*], Angela R. Laird [a], Nitin Tandon [b], Crystal Franklin [a], Jack L. Lancaster [a], Peter T. Fox [a,c]

[a] Research Imaging Institute, University of Texas Health Science Center, San Antonio, TX, USA
[b] Dept. of Neurosurgery, University of Texas Health Science Center, Houston, TX, USA
[c] Audie L. Murphy South Texas Veterans Administration Medical Center, San Antonio, TX, USA

ARTICLE INFO

Article history:
Accepted 21 April 2012
Available online 5 May 2012

Keywords:
Functional connectivity
Positron emission tomography (PET)
Supplementary motor area (SMA)
Transcranial magnetic stimulation (TMS)
BrainMap®
Meta-analytic connectivity mapping
Electrophysiological mapping
Behavioral domain

ABSTRACT

Neuro-imaging methods for detecting functional and structural inter-regional connectivity are in a rapid phase of development. While reports of regional connectivity patterns based on individual methods are becoming common, studies comparing the results of two or more connectivity-mapping methods remain rare. In this study, we applied transcranial magnetic stimulation during PET imaging (TMS/PET), a stimulation-based method, and meta-analytic connectivity modeling (MACM), a task-based method to map the connectivity patterns of the supplementary motor area (SMA). Further, we drew upon the behavioral domain meta-data of the BrainMap® database to characterize the behavioral domain specificity of two maps. Both MACM and TMS/PET detected multi-synaptic connectivity patterns, with the MACM-detected connections being more extensive. Both MACM and TMS/PET detected connections belonging to multiple behavioral domains, including action, cognition and perception. Finally, we show that the two connectivity-mapping methods are complementary in that, the MACM informed on the functional nature of SMA connections, while TMS/PET identified brain areas electrophysiologically connected with the SMA. Thus, we demonstrate that integrating multimodal database and imaging techniques can derive comprehensive connectivity maps of brain areas.

Introduction

Inter-regional connectivity is a fundamental determinant of the functional properties of any brain region (Maunsell and Van Essen, 1987). In recognition of the importance of connectivity in describing region function, considerable effort and creativity has been invested by the neuroimaging community in developing non-invasive methods for mapping inter-regional connectivity in humans. One of the earliest methods developed was the task based connectivity mapping. These mapping studies have localized the neural populations performing specific mental operations across several behavioral domains. While such connectivity mapping provides inter-regional covariances in functional activation levels during task performance (Friston et al., 1993), it suffers from important limitations. First, since the data are obtained during task performance, the true interactions between regions cannot be distinguished from the interactions between different components of a behavior (Paus et al., 1997). Second, such functional connectivity can indicate information exchange but not information flow. Therefore, developing task-independent methods of measuring inter-regional connectivity became an important technical objective of the neuroimaging community.

During the last decade, several task independent connectivity-mapping methods have been pioneered. These include: region-seeded covariance analyses of resting-state functional MRI (rsfMRI; Biswal et al., 1995; Xiong et al., 1999), independent components analysis (ICA) of rsfMRI (McKeown et al., 1998; Smith et al., 2009), tractography derived from diffusion tensor and diffusion spectroscopy MRI (DTI and DSI, respectively; Behrens and Johansen-Berg, 2005; Le Bihan, 2003; Mori and Zhang, 2006), imaging during brain stimulation (e.g., TMS/PET; Chouinard et al., 2003; Ferrarelli et al., 2004; Fox et al., 1997; Ilmoniemi et al., 1997; Komssi et al., 2004; Paus et al., 1997; Speer et al., 2003a, 2003b), and cortico-cortical evoked potentials (CCEP; Matsumoto et al., 2004, 2007; Keller et al., 2011).

Resting-state networks identified by ICA almost certainly reflect true synaptic connectivity (Fox and Raichle, 2007; Smith et al., 2009). However, the number of networks identified and their functional attributes are user defined. Further, this analysis is weighted by a prominent component, the default mode network (DMN) that characterizes the resting-state stream of consciousness (Laird et al., 2009; Smith et al., 2009). Therefore functional networks identified by ICA can include brain areas that are active during default mode. Additionally, ICA permits the identification of an ensemble of brain areas that constitute a functional network, but cannot map the

* Corresponding author at: Research Imaging Institute, 7703 Floyd Curl Drive, Mail Code 6240, University of Texas Health Science Center, San Antonio, TX 78229, USA. Fax: +1 210 567 8152.
E-mail address: narayana@uthscsa.edu (S. Narayana).

1053-8119/$ – see front matter © 2012 Elsevier Inc. All rights reserved.
doi:10.1016/j.neuroimage.2012.04.060

connectivity of a particular brain region. Imaging-based tractography, overcomes this drawback, and can not only trace large pathways, but with recent advances in the analytical methods, also trace smaller cortico-cortical networks (Johansen-Berg and Rushworth, 2009). However, information about the viability of synaptic connections and the direction of information flow—anterograde or retrograde—cannot be derived from DTI. Tract tracing and stimulation based mapping, on the other hand, can provide such information (Fox et al., 1997). Further, stimulation-based mapping has the clear advantage over task based mapping of being truly "task-independent" as the connectivity maps are uninfluenced by task-based recruitment of individual regions; rather, the displayed connectivity can be considered an electrophysiological connectivity of the stimulated region. While CCEP also fall into this category, its application is limited in that the connectivity of only a few stimulation targets can be assessed. More importantly, altered connectivity consequent to brain pathology is a significant confound of CCEP.

TMS/PET, an electrophysiological mapping technique of recording remote sites of covariant neuronal activity during TMS stimulation of a brain region, overcomes several of the drawbacks of other task-independent connectivity mapping techniques. Connectivity determined by TMS/PET can identify afferent and efferent connections, and remote excitations and inhibitions (Fox et al., 1997). Knowledge of the site of stimulation (i.e. where electric current is directly induced in the network) enables mapping direct or first order connections, as well as trans-synaptically mediated secondary and tertiary connections (Laird et al., 2008). Connectivity mapping using TMS/PET provides the whole brain connectivity of the stimulated area and can be readily performed on healthy volunteers.

However, connectivity maps derived from task independent methods including TMS/PET do not indicate the functional nature of the stimulated and the connected areas. Current meta-analytic connectivity mapping (MACM) techniques are task-general in that they draw upon the wide range of tasks compiled in a meta-analysis or archived in neuroimaging databases (Cauda et al., 2011; Robinson et al., 2009)—rather than being task specific (in the manner of an activation likelihood estimate (ALE) map of an individual task) or task independent (in the manner of TMS/PET). In this context, MACM has the salient advantages of: 1) utilizing extremely large datasets; and 2) using meta-data to characterize the functional contributions of specific connections. For these reasons, the combination of TMS/PET and MACM seems particularly apt for investigating the electrophysiological inter-regional connectivity of a region and to outline its functional connectivity. To investigate the feasibility of this strategy, we used the combination of TMS/PET and MACM to investigate the connectivity of the human supplementary motor area (SMA).

Despite its diminutive eponym, the SMA has emerged as a significant contributor to motor behavior. A higher-order role for this "supplementary" region was suggested in the original reports by Foerster (1936) and Penfield and Welch (1951), who noted speech disruption and complex movements during stimulation, rather than the simple muscle contractions elicited by stimulation of primary motor cortex. A higher-order role of SMA in the motor network was confirmed and extended by the earliest functional imaging reports of SMA activation, in which it was observed to be engaged even during internally generated (i.e. no stimulus being presented), non-motor (i.e., with no over movements performed) tasks (Orgogozo and Larsen, 1979; Roland et al., 1980). Since that time, hundreds of functional imaging studies have reported task-induced activation of the SMA in association with an enormous repertoire of tasks, even those requiring no overt or covert movement.

In addition to its role in limb motor behavior, SMA has also been shown to be involved in speech production (Fiez and Petersen, 1998; Penfield and Welch, 1951; Price, 2010), sensory discrimination (Chung et al., 2005; Liu et al., 1999; Van de Winckel et al., 2005), rhythm and beat perception (Grahn and Brett, 2007; Peretz et al., 2009), sensori-motor integration, and orienting processes (Picard and Strick, 2003; Wiesendanger and Wiesendanger, 1985a). A growing body of reports has shown that the SMA is important in motor learning (Doyon and Benali, 2005; Doyon et al., 2009). Collectively, these findings suggest that SMA is an important component of behavioral domains that are non-motor.

In the present study, we tested the following hypotheses: 1. the electrophysiological connectivity of the human SMA can be successfully mapped by TMS/PET, and that these connections will be comparable to those derived from tract tracing in non-human primates; 2. the functional connectivity map of SMA derived by MACM will demonstrate a significant overlap with the electrophysiological map, with MACM demonstrating a broader connectivity pattern; 3. behavioral meta-data indexed in the BrainMap database can be used to assign functional attributes to the electrophysiological connectivity map; and 4. if SMA plays an important role in non-motor behaviors, then it should be reflected in its electrophysiological connectivity map. In order to examine these hypotheses, the electrophysiological connectivity of SMA was mapped by TMS/PET and its functional connectivity was mapped by MACM utilizing the BrainMap database (www.BrainMap.org). The behavioral meta-data information in the BrainMap database was used to functionally characterize the meta-analytic and electrophysiological connectivity maps. Finally, we generated MACMs for the behavioral sub-domains of action, perception, cognition, emotion, and interoception in order to investigate further the role of SMA in non motor behaviors.

Methods

Electrophysiological connectivity of the right SMA mapped by TMS/PET

Participants

Ten, right-handed, healthy normal volunteers (4 men; 6 women) with a mean age of 32.5 years (age range: 20–43 years) participated in the study after approval by the institutional review board, and the radiation safety committee at the University of Texas Health Science Center at San Antonio. Informed consent was obtained from all participants in accordance with the declaration of Helsinki.

Identification of SMA for TMS targeting

For purposes of targeting the SMA, a quantitative meta-analysis of functional imaging studies was carried out in which healthy volunteers performed a finger-tapping task. This strategy emulated the meta-analysis-based, probabilistic strategy introduced by Paus et al. (1997). The meta-analysis in the present study was limited to experiments entered in the BrainMap database that imaged isolated tapping of the left index finger, a task that recruits the first dorsal interosseous muscle (FDI). A total of 54 foci from 37 experiments reported in fifteen studies met these criteria (Table 1). Using these foci, an ALE was performed in Talairach space using GingerALE 2.0 (www.BrainMap.org). Coordinates originally published in MNI space were converted to Talairach space using the Lancaster (icbm2tal) transformation (Lancaster et al., 2007). In order to determine only the most strongly activated regions, the resultant ALE map was thresholded to a cluster size $> 150\ mm^3$ (random effects analysis; Eickhoff et al., 2009a) and a false discovery rate (FDR, $q = 0.005$) corrected threshold of $p < 0.0003$ (Laird et al., 2005). The locations of $M1_{hand}$ and SMA_{hand} as identified by this analysis were at Talairach coordinates of (36, −18, 54) and (6, −4, 52) respectively (Fig. 1). SMA on average was noted to lay 14 mm anterior to $M1_{hand}$ and 6 mm lateral to the midsagittal plane. Thus, SMA was targeted in a probabilistic, semi-stereotactic manner, using $M1_{hand}$ as an internal functional landmark.

TMS targeting and delivery

TMS was applied to the right $M1_{hand}$ area while the motor evoked potentials (MEP) in the left first dorsal interosseous was monitored

Table 1
Studies included in the ALE meta-analysis performed to identify the stereotactic location of right SMA in relation to the right primary motor cortex.

Author	Number of subjects	Task
Colebatch et al. (1991)	6	Thumb opposition vs rest
Seitz and Roland (1992)	9	Finger sequence vs rest
Sadato et al. (1997)	12	Mirror movement vs rest
	21	Parallel movements vs rest
Samuel et al. (1997)	6	Bimanual vs rest
Catalan et al. (1998)	13	Finger sequence vs rest
Goerres et al. (1998)	6	Finger press vs rest
Gelnar et al. (1999)	8	Finger tapping vs rest
Joliot et al. (1999)	8	Finger tapping vs rest
Gerardin et al. (2000)	8	Finger tapping vs rest
Jäncke et al. (2000)	11	Left vs right finger tapping
Seitz et al. (2000)	6	Bimanual vs rest
	12	Finger tapping imagery vs rest
Indovina and Sanes (2001)	9	Finger tapping vs rest
Koski et al. (2002)	14	Contralateral vs ipsilateral
Haslinger et al. (2002)	8	Finger tapping vs rest
Lacourse et al. (2005)	54	Novel/skilled vs rest

by electromyography. The resting motor threshold (rMT) was determined as the minimum stimulus intensity that produced a MEP greater than 100 μV in 50% of trials during complete muscle relaxation (Rossini et al., 1994), and the scalp location of $M1_{hand}$ was marked. The location of SMA_{hand} in each individual was then localized as lying 14 mm anterior to $M1_{hand}$ and 6 mm to the right of midline. To stimulate the medial surface of the hemisphere, the TMS coil was oriented with the E-field oriented normal to the midsagittal plane (B-ear orientation), following the cortical columnar cosine principle (Fox et al., 2004). To hold the coil rigidly in the proper location and orientation, a robotic, TMS holding system was used (Lancaster et al., 2004).

TMS was delivered during PET using a water-cooled figure-8 coil powered by a Cadwell HSMS unit (Cadwell, Inc.; Kennewick, Washington) at intensities of 75%, 100% and 125%, relative to rMT. A 3 Hz train of TMS delivered for 120 s prior to tracer injection and continued during the first 40 s after the arrival of radiotracer in the brain. For the auditory control for TMS clicks during rest scans we used a second TMS coil mounted approximately 12 in. behind the treatment coil and not in contact with the scalp. The machine output to the auditory-control coil was adjusted until the sound pressure level measured at the external auditory meatus was the same as that during the 100% rMT TMS condition. Auditory-control TMS was delivered at 3 Hz for the same duration as during the TMS conditions.

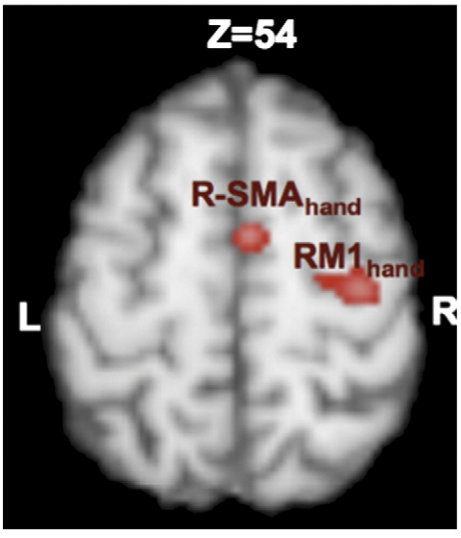

Fig. 1. Localization of SMA in relation to the right M1 derived from ALE analysis of BrainMap database. The center-of-mass of the $RM1_{hand}$ activation was at (36, −18, 54) and that of R-SMA_{hand} was at (6, −4, 52).

PET image acquisition

Participants were scanned in a Scanditronix/GE 4096WB PET scanner in 2D mode (pixel spacing 2 mm, spatial resolution 6.5 mm full width at half maximum (FWHM) in the axial plane, inter plane center to center distance 6.5 mm; scan planes 15; z-axis field of view (FOV) 10.5 cm). Cerebral blood flow (CBF) was measured using $H_2^{15}O$, administered as an intravenous bolus of 1850–2775 MBq/injection (Fox et al., 1984). Ninety seconds of scanning was triggered as the tracer bolus entered the brain and TMS, auditory-control TMS, or hand movement were performed during the first 40 s. Each participant underwent 6 scans during TMS stimulation (2 trials/intensity), one scan during voluntary hand movement, and 2 scans of rest with auditory stimulation. The order of scan conditions was randomized across participants.

MRI image acquisition

Anatomical MRI was acquired in each participant and used to optimize spatial normalization. MR imaging (1.9 T, Elscint Prestige) was performed using a high resolution, 3-D GRASS sequence TR = 33 ms; TE = 12 ms; flip angle = 60°; voxel size = 1 mm^3; matrix size = 256 × 192 × 192.

PET and MRI image pre-processing

Images were reconstructed into 60 slices, each 2 mm thick and with an image matrix size of 60 × 128 × 128, using a 5 mm Hann filter resulting in images with a spatial resolution of approximately 7 mm (full-width at half-maximum (FWHM)). PET images were value normalized to a whole-brain mean of 1000 counts. All MRI and PET data were corrected for motion and spatially normalized to the Talairach coordinate system (Talairach and Tournoux, 1988) using spatial normalization algorithms (Kochunov et al., 1999; Lancaster et al., 1995) and co-registered using the Convex Hull algorithm (Lancaster et al., 1999). Of the ten participants imaged, one participant's images had serious motion artifacts that could not corrected, and two additional participants did not complete the MRI, and were eliminated from further analysis.

Conditional contrast analysis

Group statistical parametric images of z scores (SPI{z}) were computed with the MIPS™ software package (Fox et al., 1984; RII, UTHSCSA, San Antonio, Texas) and anatomically labeled using the Talairach Daemon (Lancaster et al., 2000). The SPI{z} contrasted 1) voluntary finger movement vs. rest during sham TMS, 2) all 3 TMS conditions (75% rMT, 100% rMT and 125% rMT) pooled vs. rest during sham TMS, and 3) each TMS intensity condition vs. rest during sham (75% rMT vs. sham; 100% rMT vs. sham; and 125% rMT vs. sham). The SPI{z} image of finger movement contrasted with the rest scan was used to identify the site of maximal SMA response during voluntary movement (Fig. 2). The SPI{z} of all TMS conditions contrasted with rest during sham TMS was used to identify the site of SMA with maximal response for TMS stimulation (Fig. 2) and to establish the location for a seed volume for voxel-wise covariance analysis. The individual TMS intensity conditions contrasted with sham TMS condition were used to characterize the CBF response at the site of stimulation. The CBF response at SMA to increasing TMS intensities was indexed by intensity of activation (z score), and the volume of activation (Table 2).

Connectivity mapping by covariance analysis

The SMA location with maximal response for TMS stimulation was found to be at Talairach co-ordinates of (8, −6, 50) and identified as the seed location for covariance analysis. The covariance of rest of the brain voxels to this SMA seed across the 3 TMS intensities and sham TMS condition was computed voxel-wise, and a SPI{r} map was

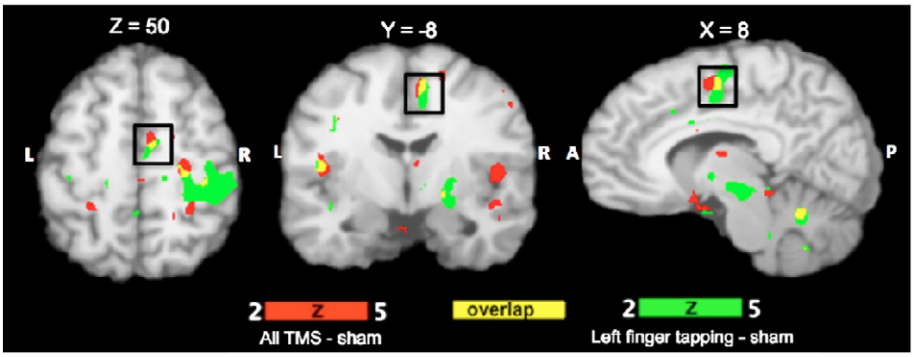

Fig. 2. Confirmation of targeting of SMA by TMS. SMA activation during TMS stimulation (red) shows good overlap (yellow) with SMA activation during a left index finger tapping (green). Conditions were contrasted with sham and rest conditions respectively and thresholded to FDR corrected $p<0.002$. The images are in Talairach coordinates.

generated. Such a correlational analysis is based on the principle that SMA and brain areas connected to the SMA are moderated by the TMS intensity in a similar manner. Thus CBF response at each of the 3 TMS conditions (75% rMT, 100% rMT, and 125% rMT) as well as the rest during sham condition (0% rMT) was used in this analysis. Prior to computation of the SPI{r}, each scan was normalized by voxel-wise subtraction of the block-average. SPI{r} were analyzed voxel-wise for correlation with the intensities of SMA seed volume ($2.7\ cm^3$) across the four conditions (0% rMT, 75% rMT, 100% rMT, and 125% rMT) by an omnibus (whole-brain) test. If the omnibus significance was proven, then a post hoc (regional) test was done and local extrema were identified (Fox et al., 2000). The SPI{r} were converted to SPI{z}, and P values were assigned from the Z distribution and corrected for the number of positive extrema. The extrema locations were anatomically labeled using the Talairach Daemon (Lancaster et al., 2000). All images were visualized using the multiple image analysis GUI (MANGO) tool (http://ric.uthscsa.edu/mango/). The brain regions found to significantly co-vary with the R-SMA are tabulated in Table 3 and shown in Fig. 3.

Meta-analytic connectivity of the right SMA

We performed a MACM analysis using the BrainMap database. Such an analysis requires a brain region of interest to be identified as the seed region within the BrainMap database. Then the entire database of neuroimaging papers is queried to determine which studies reported activation within the given seed region. Coordinates of all activations reported in these papers are then downloaded, and meta-analytic statistics are computed to determine regions of the brain that were co-activated with the seed region (Robinson et al., 2009). In the present study, we used the location of SMA identified in the TMS/PET study as the seed region. This location was very similar to the probabilistic location of the right-SMA derived from other meta-analytic studies (Mayka et al., 2006; Picard and Strick, 1996) and cyto-architecture (Eickhoff et al., 2007). A cubic seed region (volume = $2.7\ cm^3$) representing the right SMA was centered at Talairach coordinates of (8, −6, 50), representing its peak location. The complete BrainMap database was searched using the following criteria: studies that enrolled normal subjects, the experimental context of normal mapping, and only activations identified by conditional contrasts. A total of 3816 foci reported in 266 experiments in 187 papers that met the above search criteria were identified. The ALE was performed on the co-ordinates of brain regions identified by the above search in Talairach space. Coordinates originally published in MNI space were converted to Talairach space using the Lancaster (icbm2tal) transformation (Lancaster et al., 2007). In order to determine only the most strongly activated regions, the resultant ALE map was thresholded to a cluster size > $936\ mm^3$ (random effects analysis; Eickhoff et al., 2009a) and a false discovery rate (FDR, $q = 0.005$) corrected threshold of $p<0.0003$ (Laird et al., 2005). The brain regions identified to be co-varying with SMA under all the behavioral domains are listed in Table 4 and shown in Fig. 4.

Table 2
The cerebral blood flow response at SMA to increasing TMS intensity. Volume of activation and the intensity of activation for each intensity contrasted with sham condition, and the peak location of SMA are listed.

Conditional contrast	x	y	z	Volume of activation (mm^3)	Intensity of activation (Z score)
75% MT-sham	7	−6	50	200	2.52
100% MT-sham	18	−6	54	752	2.89
125% MT-sham	8	−6	50	1056	2.70

Comparison between TMS/PET and MACM connectivity

Spatial overlap

Connectivity maps derived from TMS/PET and SMA MACM were examined for spatial similarity by using Pearson spatial cross-correlation (FSL, www.fmrib.ox.ac.uk/fsl/; Smith et al., 2009). The spatial correlation between the two maps was $r = 0.39$. We applied Fisher's r-to-z transform using a conservative degrees-of-freedom value of 500 (number of independent resolution elements, Smith et al., 2009) and converted the resultant z score to a P value. Using this method, we found that the connectivity maps derived from TMS/PET and MACM were significantly correlated ($p<0.0001$). Another analysis was performed to compare the regional overlap between the electrophysiological and functional connectivity of the human SMA, where we compared the strengths of the connection (r value in TMS/PET and the ALE score in MACM) in brain areas that were common to both the covariance analysis of TMS/PET (listed in Table 3) and the MACM analysis (listed in Table 4). To allow a direct comparison, and to account for different measures of the connection strength displayed in Table 3 (r values) and Table 4 (ALE scores), the values were normalized to their respective maximum score (Fig. 5).

Behavioral domain profile overlap

In BrainMap, meta-data are included on the cognitive, perceptual, or motor process isolated by the statistical contrast. The domain of behavioral system is classified according to six main categories and their related subcategories: cognition, action, perception, emotion, interoception, or pharmacology (a complete list of BrainMap's behavioral domains can be accessed at http://BrainMap.org/scribe/). We analyzed the behavioral domain (BD) meta-data associated with the two connectivity maps to determine the frequency of domain "hits" relative to its distribution across the whole brain (i.e., the entire

Table 3
Locations of peak extrema (x, y and z in Talairach co-ordinates), volumes, r value, and p values of brain regions co-varying with the right SMA during TMS stimulation. The behavioral domains under which the brain areas were found to be functionally connected with the SMA are also indicated. A: action, P: perception, C: cognition, E: emotion and I: interoception. Identifying modality: E: electrophysiological mapping, M: meta-analytic connectivity mapping.

x	y	z	Region	Brodmann area	Volume (mm^3)	R	p	Behavioral domain	Identifying modality
6	−10	56	SMA	6	824	0.805	0.001	APCEI	
6	−62	−30	Cerebellum-uvula		464	0.618	0.007	ACP	E, M
38	16	8	Insula	13	336	0.66	0.004	AP	E, M
−12	−80	−32	Cerebellum-uvula		656	0.693	0.003	AC	E, M
−34	−11	42	Dorsal premotor cortex	6	272	0.674	0.004	AC	E, M
−57	−56	28	Superior temporal gyrus	39	408	0.668	0.004	AC	E, M
−36	−70	−30	Cerebellum-tuber		648	0.664	0.004	AC	E, M
−34	−65	−10	Cerebellum-declive		224	0.638	0.006	AC	E, M
52	−4	46	Dorsal premotor cortex	6	264	0.632	0.006	AC	E, M
−2	−64	64	Precuneus	7	520	0.628	0.006	AC	E, M
−59	−12	30	Precentral gyrus	4	272	0.602	0.009	AC	E, M
25	−22	68	Precentral gyrus	4	224	0.659	0.005	A	E, M
−62	−20	30	Postcentral gyrus	2	224	0.622	0.007	A	E, M
68	−20	20	Postcentral gyrus	40	400	0.747	0.002	P	E, M
−53	10	34	Middle frontal gyrus	9	368	0.676	0.004	C	E, M
−63	−48	−2	Middle temporal gyrus	21	272	0.664	0.004	C	E, M
69	−23	4	Superior temporal gyrus	41	312	0.611	0.008	P	E, M
4	−50	60	Precuneus	7	760	0.727	0.002		E
42	38	28	Superior frontal gyrus	9	312	0.656	0.005		E
29	51	35	Superior frontal gyrus	9	392	0.631	0.006		E
45	30	34	Middle frontal gyrus	9	208	0.627	0.007		E
32	44	−4	Middle frontal gyrus	10	224	0.614	0.008		E
2	−93	−10	Lingual gyrus	18	264	0.63	0.006		E
18	−60	18	Posterior cingulate	31	216	0.684	0.003		E
27	−84	16	Middle occipital gyrus	19	216	0.689	0.003		E
4	−2	50	SMA	6	840	0.798	0.001	Direct spread	E
−10	−8	58	SMA	6	464	0.71	0.002	Direct spread	E
−2	6	48	Pre-SMA	6	672	0.721	0.002	Direct spread	E
−14	−18	69	Precentral gyrus/M1Leg	4/6	416	0.705	0.003	Direct spread	E
6	−42	60	Paracentral lobule	5	536	0.669	0.004	Direct spread	E
8	19	65	Superior frontal gyrus/frontal eye field	6	248	0.664	0.004	Direct spread	E
9	2	68	Pre-SMA	6	480	0.65	0.005	Direct spread	E
			Superior frontal Gyrus/supplementary						
2	16	48	Eye field	8	600	0.645	0.005	Direct spread	E
7	14	64	Pre-SMA	6	408	0.639	0.006	Direct spread	
5	3	11	Caudate		40	0.535	0.017	AC	E, M
−16	−34	12	Thalamus		16	0.52	0.02	AP	E, M

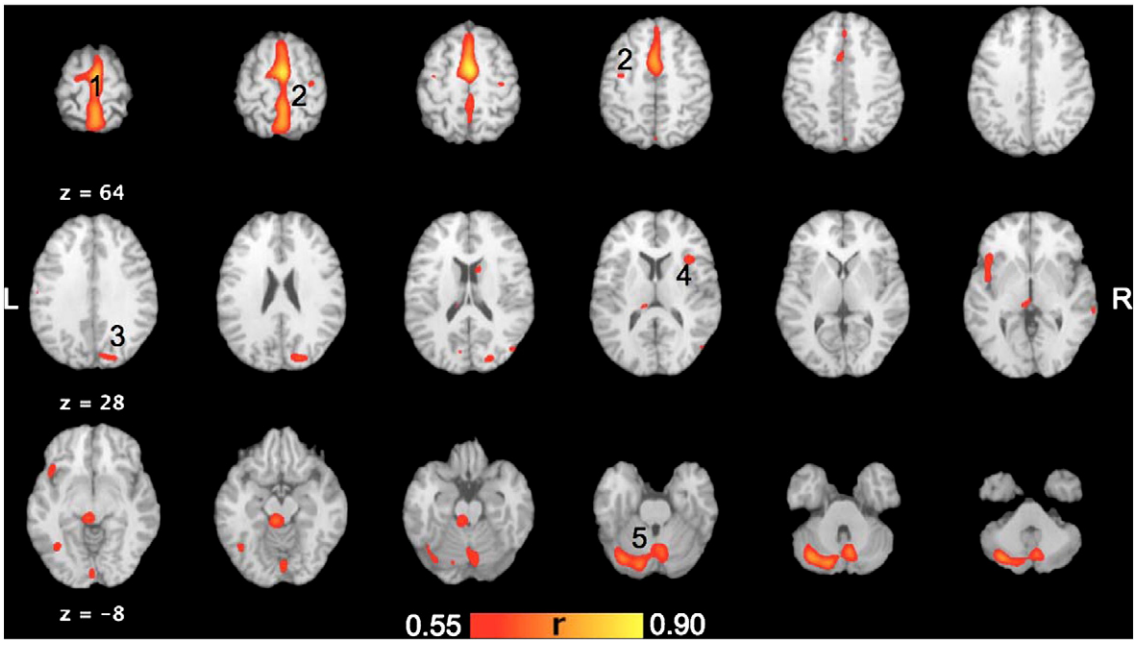

Fig. 3. Brain regions co-varying with the right SMA as determined by task independent method TMS/PET (FDR corrected $p<0.009$). Medial (1) and lateral (2) motor areas in the frontal lobe, the right parietal cortex (3), the right insula (4) and cerebellum (5) showed covariance with R-SMA. The images are in Talairach coordinates.

Table 4
Locations of peak extrema and their ALE scores of brain regions identified by MACM.

ALE score	Talairach coordinates			Region	Brodmann area
	x	y	z		
0.609	2	−4	52	Medial frontal gyrus, supplementary motor area	6
0.173	24	−10	54	Dorsal premotor cortex	6
0.100	48	−2	34	Dorsal premotor cortex	6
0.136	34	−22	56	Precentral gyrus	4
0.119	50	4	16	Inferior frontal gyrus	44
0.153	−26	−12	56	Dorsal premotor cortex	6
0.114	−50	2	30	Dorsal premotor cortex	6
0.071	−50	−10	30	Dorsal premotor cortex	6
0.144	−34	−12	50	Precentral gyrus	4
0.079	−48	2	14	Inferior frontal gyrus	44
0.106	−34	18	4	Insula	13
0.123	36	−46	48	Inferior parietal lobule	40
0.088	54	−24	22	Postcentral gyrus	40
0.107	−28	−56	46	Superior parietal lobule	7
0.082	−50	−28	26	Inferior parietal lobule	40
0.107	−40	−38	40	Inferior parietal lobule	40
0.106	−38	−30	50	Postcentral gyrus	3
0.093	−52	−18	8	Superior temporal gyrus	41
0.064	52	−20	8	Superior temporal gyrus	41
0.143	12	−18	8	Thalamus	
0.100	22	2	8	Putamen	
0.134	−14	−18	8	Thalamus	
0.113	24	−58	−14	Cerebellum	
0.086	2	−56	−14	Cerebellum	
0.103	−14	−60	−8	Cerebellum	
0.088	−30	−46	−30	Cerebellum	
0.074	−24	−56	−24	Cerebellum	

database). The behavioral domain and sub-domain meta-data tabulated in the BrainMap database were used to create 3-D images, one for each of the fifty-one behavior sub-domains with activation foci tallied at corresponding Talairach coordinates. These data were then

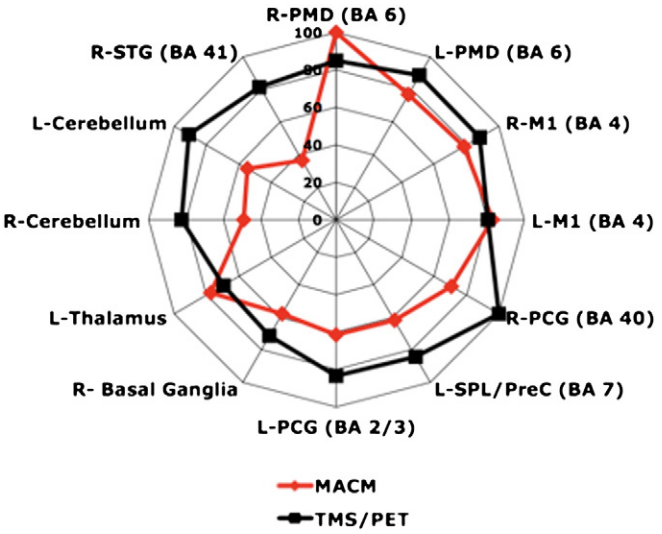

Fig. 5. Spatial overlap between MACM and TMS/PET connectivity maps. Brain areas that were observed to be co-varying (TMS/PET) or co-activating (MACM) with the SMA. The ALE scores (MACM) and the correlation values (TMS/PET) were normalized to the maximum value in each map, to demonstrate the relative strengths of connections. R—right, L—left, PMD—dorsal premotor cortex, M1—primary motor cortex, PCG—post central gyrus, SPL—superior parietal lobule, PreC—precuneus, STG—superior temporal gyrus.

queried using TMS/PET and MACM spatial maps. Activations within the TMS/PET and MACM spatial maps (that included all the significant activations) for each behavior sub-domain image were tallied to formulate a behavioral profile for each spatial map. To correct for differences in the number of reported activations in the sub-domains in the database, we converted activation tallies to activation fractions (p_o, ROI tally/whole-brain tally) for each behavior sub-domain. We chose the reference probability (p_r) as that which would occur if activation foci were uniformly distributed throughout the brain, i.e. not localized. The difference between observed and reference activation probabilities ($p_o - p_r$) served as the basis for the relevance measure.

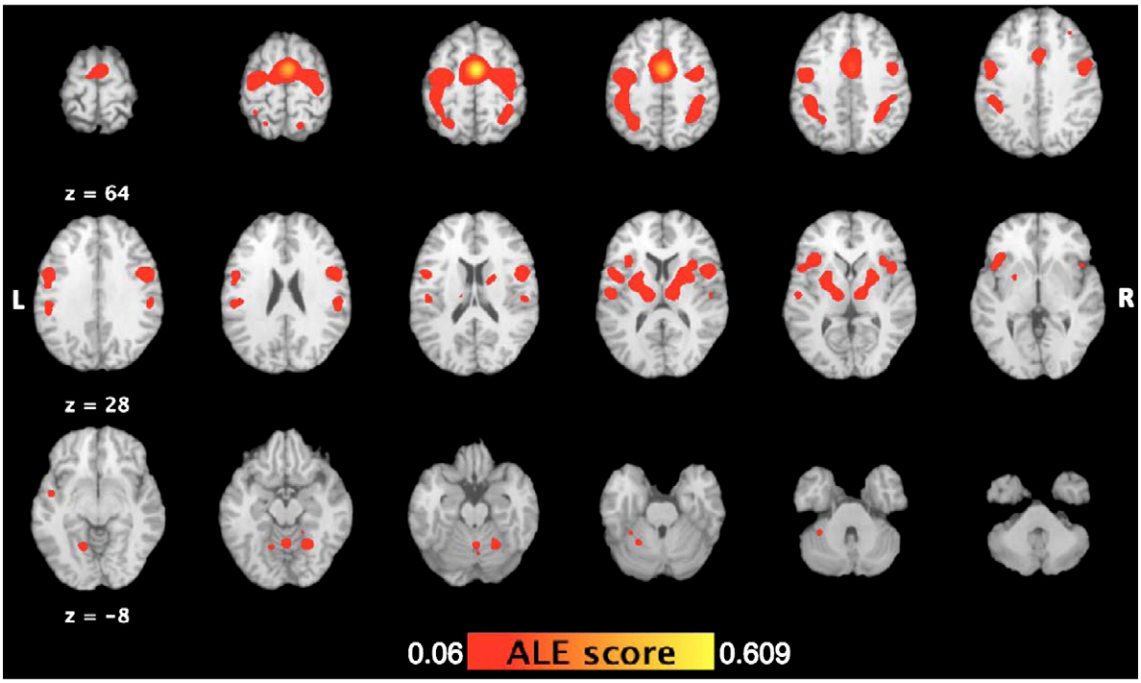

Fig. 4. Brain regions co-varying with the right SMA as determined by domain independent MACM analysis. Behavioral domains included were action, cognition, perception, and emotion and interoception. The images are in Talairach coordinates.

To provide a means to standardize the behavior relevance measure and account for its variance by sub-domain we formulated a relevance z-score. The binomial distribution was used to estimate variances for p_o and p_r since it models two-outcome events where observed or expected activations fall either inside or outside of the ROI. The binomial distribution can be used to calculate variances if the probability of success (p) and the number of trials (n) is known. In this study p_o and p_r were the observed and reference "success" probabilities (probability of activations falling within the TMS/PET and MACM ROIs), and the number of trials was the whole-brain activation tally (N_b) for a sub-domain. The variance of p_o was estimated as $s_o^2 = p_o(1-p_o)/N_b$ and similarly that of p_r as $s_r^2 = p_r(1-p_r)/N_b$. Relevance z-scores were formulated as follows:

$$z = \frac{p_o - p_r}{\left(\frac{p_o(1-p_o)+p_r(1-p_r)}{N_b}\right)^{1/2}}. \quad (1)$$

Relevance z-scores were calculated for all fifty-one sub-domains, but only those with z-scores > 3.0 are considered significant and reported here (Bonferroni corrected to overall p-value of 0.05). This algorithm is incorporated as a plugin in the Mango software (behavioral profiling, Mango plugin, http://ric.uthscsa.edu/mango/). The z scores of each behavioral sub-domain for the MACM and the TMS/PET maps are plotted in Fig. 6.

Domain-specific meta-analytic connectivity of the right SMA

In order to further investigate the role of SMA in non-motor domains, the BrainMap database was searched separately for brain regions co-activated with the SMA seed volume under the behavioral domains of action, perception, and cognition that also met the criteria of normal subjects under diagnosis, and normal mapping context. The behavioral domains of emotion and interoception were combined for this analysis as very few experiments reported SMA activation individually under these domains, and the two domains recruit brain areas that greatly overlap (Laird et al., 2011a). This analysis was restricted to experiments coded only under a single domain and specifically experiments that were coded across multiple domains were rejected. Thus we eliminated the possibility that co-activation of SMA under perceptual, cognitive, and emotional and interoceptive domains could merely be due to the concomitant motor task. Similarly, we ensured that co-activation of parietal, prefrontal and temporal areas in the action domain could not be from simultaneous performance of perceptual and cognitive tasks. This search identified 86 experiments under action, 46 experiments under cognition, 21 experiments under perception, and 8 experiments under emotion and interoception that reported SMA activation. ALE analysis was performed on these subsets and thresholded for FDR $q < 0.05$. The brain regions that were found to be common across domains, and those seen only in individual domains are shown in Fig. 7. We also performed the Pearson cross correlation analysis (FSL, www.fmrib.ox.ac.uk/fsl/; Smith et al., 2009) and compared the spatial correlation between each of the domain specific maps with TMS/PET map.

Meta-analytic connectivity of the left SMA

To investigate if the connectivity pattern observed for the right SMA could be extended to the left SMA, we generated a MACM of the left SMA using the same criteria as for the right SMA. A cubic VOI (volume = 2.7 cm^3) representing the left SMA was centered at Talairach coordinates of $x = -8$, $y = -6$ and $Z = 50$, representing its peak location. The complete BrainMap database was searched using the following criteria: studies that enrolled normal subjects, the experimental context of normal mapping, and only activations identified by conditional contrasts. A total of 4134 foci reported in 235 experiments in 179 papers that met the above search criteria were identified. The ALE was performed on the co-ordinates of brain regions identified by the above search in Talairach space. Coordinates originally published in MNI space were converted to Talairach space using the Lancaster (icbm2tal) transformation (Lancaster et al., 2007). In order to determine only the most strongly activated regions, the resultant ALE map was thresholded to a cluster size > 900 mm^3

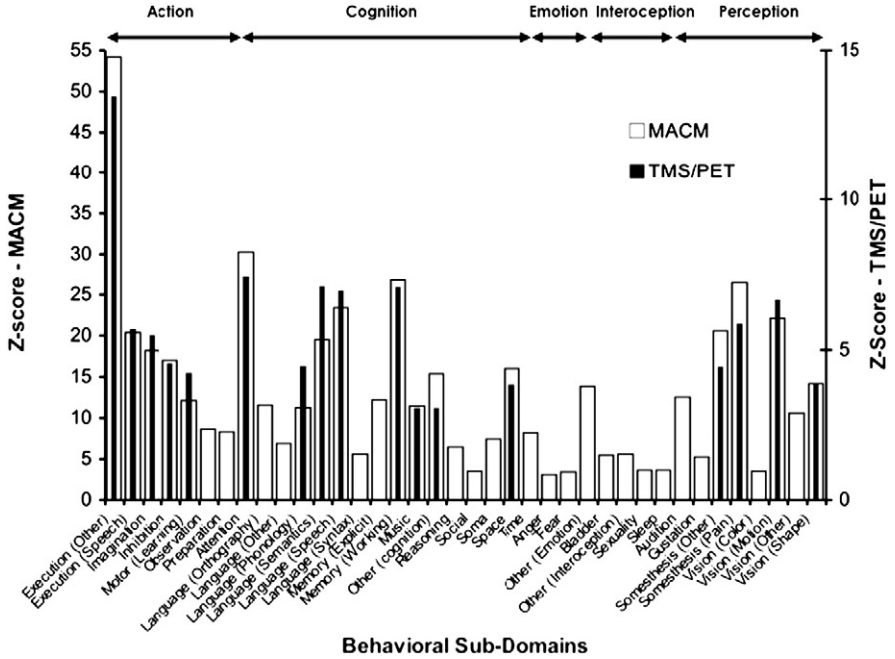

Fig. 6. Behavioral profile analysis of MACM (white bars) and TMS/PET (black bars) connectivity maps. The y-axis represents the z-scores (> 3, corrected) of the sub-domains for MACM analysis (left axis) and TMS/PET (right axis). Brain areas in the MACM map are represented in several behavioral sub-domains that spanned across action, cognition, emotion, interoception, and perception. The behavioral domains represented in the TMS/PET map are limited to few sub-domains in action, cognition, and perception.

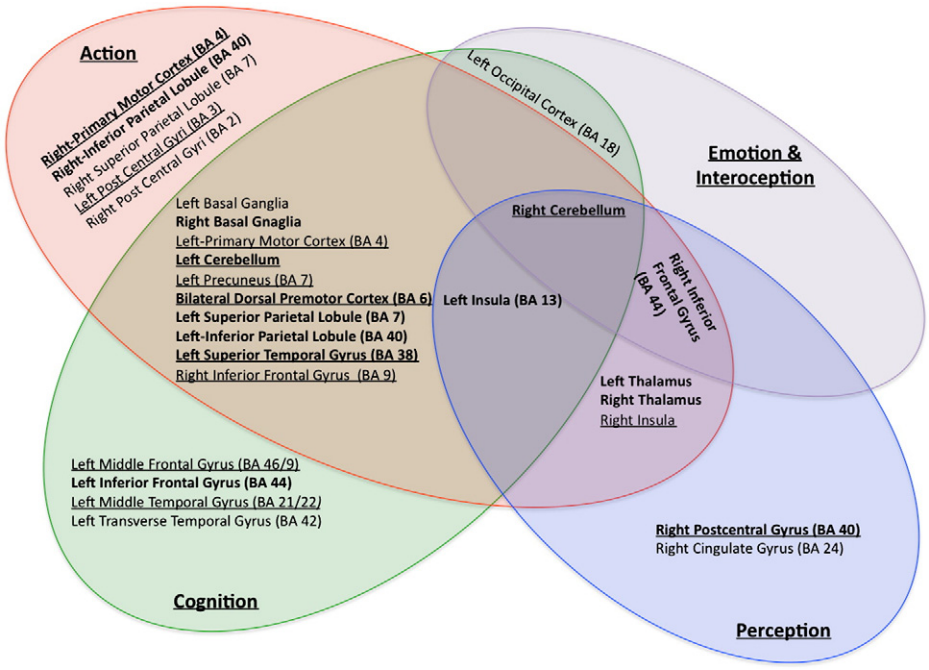

Fig. 7. Brain regions co-varying with the right SMA as determined by domain specific MACM analysis under behavioral domains of action (red), cognition (green), perception (blue), and emotion combined with interoception (purple). Brain areas overlapping for these functional domains are listed in the center (right cerebellum). Additionally, brain regions that co-activated with SMA common to three domains, two domains, and under each domain are also listed. The brain regions in bold font were also identified by domain general MACM. The regions underlined were identified by TMS/PET.

(random effects analysis; Eickhoff et al., 2009a) and a false discovery rate (FDR, $q = 0.005$) corrected threshold of $p < 0.0003$ (Laird et al., 2005). The brain regions identified to be co-varying with the left SMA under all the behavioral domains are shown in Fig. 8.

Results

Task independent connectivity mapping using TMS/PET

TMS targeting

Average rMT of 7 participants was $68 \pm 7.8\%$ machine output (range 62–80%). All subjects tolerated TMS without any adverse effects. Localization of SMA in relation to the right M1 derived from ALE analysis of BrainMap database is shown in Fig. 1. The center of activation of $RM1_{hand}$ was (36, −18, 54) and that of $R\text{-}SMA_{hand}$ was at (6, −4, 52). The accurate targeting of SMA was confirmed by comparing the location of SMA in the finger tapping task and TMS stimulation (Fig. 2). There was significant overlap in the SMA locations (shown in yellow in Fig. 2) observed during finger tapping (shown in green in Fig. 2; peak location (9, −12, 56)) and TMS stimulation (shown in red in Fig. 2; peak location at (8, −6, 50)) conditions. This provided the evidence that we stimulated SMA in all subjects and the location of SMA derived from contrasting all TMS conditions with sham is representative of SMA_{hand} area in humans.

Response of SMA to increasing TMS intensities

We characterized the local response to TMS by measuring the z scores and the volume of activation at SMA for each TMS intensity. The location of activation was similar for all three intensities, with the location of activation for 100% rMT being more lateral. The strength of activation as measured by z score at 75% rMT was 2.52, and increased to 2.89 at 100% rMT. The z score plateaued at 125% rMT and remained at 2.70. However the volume of activation increased with increasing TMS intensity (see Table 2). Thus, it appears that SMA was maximally stimulated at 100% rMT, and further increases in TMS intensity resulted in stimulation of nearby areas.

Connectivity of SMA derived from TMS/PET

The TMS enhanced connectivity of the SMA is depicted as a voxel-wise covariance image generated using SMA targeted by TMS as the region of interest. Regions with the high covariance were assumed to be the ones most strongly connected with the SMA. Regions with an r-value of ≥ 0.4 at a significance level of $p \leq 0.009$ and volume $> 150\ mm^3$ (equal to $p \leq 0.05$ corrected for FDR) were

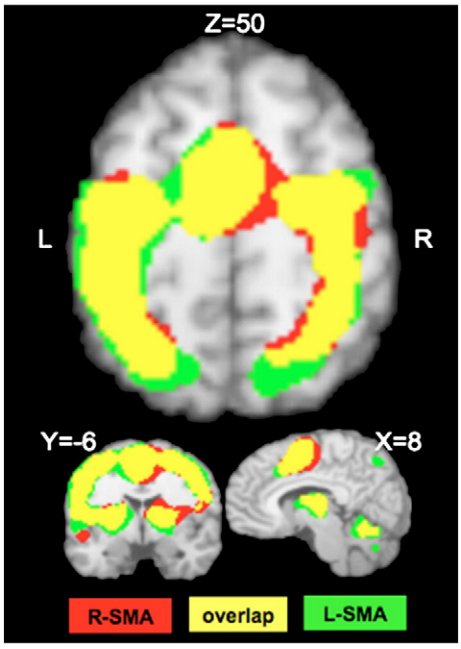

Fig. 8. Comparison of MACMs of the right (red) and the left (green) SMA, and its significant overlap (yellow). The two MACMs had a Pearson's correlation of 0.8 ($p < 0.0001$).

considered significant and evaluated further. Regions that co-varied with the SMA are reported below and listed in Table 3 and represented in Fig. 3.

Activity in the right SMA was found to strongly positively covary with all other parts of the right SMA and pre SMA (Table 3 and Fig. 3). Positive covariance was also seen with the frontal lobe at the posterior border of the SMA, adjoining primary leg motor cortex and with the mesial superior frontal lobe anterior to the SMA, Brodmann area (BA; Brodmann, 1905) 8b. Correlations were also seen with the right $M1_{hand}$ (BA 4), the left $M1_{mouth}$, bilateral dorsal premotor cortices (PMd), and bilateral prefrontal areas (BA 9 and BA 10).

SMA activity co-varied with the activity in the left primary sensory cortex (S1; BA 2), bilateral inferior parietal lobule (IPL), and precuneus (BA 40 and BA 7). In addition, R-SMA co-varied with ipsilateral posterior cingulate (BA 31) as well. Positive covariances were seen with the >bilateral superior and middle temporal gyri (BA 21/22 and BA 39), and anterior and posterior aspects of ipsilateral insula. A positive covariance of the right SMA was noted with the middle occipital gyrus (BA 19) and with lingual gyrus (BA 18). Cerebellar connections were predominantly left sided, but the right cerebellum also co-varied with the SMA. Correlation of SMA activity with both thalamus and basal ganglion did not reach significance levels (see Table 3).

Meta-analytic connectivity of SMA

The overall connectivity map of the SMA represents mainly an aggregate of brain regions that co-activate with SMA during action, perception, cognition, emotion and interoception. The brain regions that co-varied with the SMA VOI across these behavioral domains are tabulated in Table 4 and shown in Fig. 4. The average Talairach location of the SMA across all experiments that were included in this analysis fell well within the VOI at (4, −5, 51). Co-activations were noted in bilateral frontal, parietal, and temporal lobes, as well as sub-cortical regions, and the cerebellum. These regions included bilateral PMd (BA 6), primary motor cortex (M1; BA 4), and ventral premotor areas (BA 44) in the frontal bole. In the parietal lobe, SMA co-activated with the left S1 (BA 3) as well as bilateral superior (BA 7) and inferior (BA 40) parietal lobules. Additionally, the left insula, the right putamen, bilateral thalami, and bilateral superior temporal gyri were co-activated with R-SMA, along with multiple locations in bilateral cerebellum (Fig. 4, Table 4).

Comparison of MACM and TMS/PET

Spatial overlap

The volumes of significant activations in the MACM and TMS/PET showed overlap, with a Pearson correlation of 0.39 ($p<0.0001$). Of the regions that were found in both maps to be significantly connected with the SMA, we found several regions common to the two methods and included bilateral PMd, M1, and cerebellum. In addition, precentral gyrus, superior temporal gyrus, and basal ganglia on the right side and precuneus and thalamus on the left side were seen to be common to both maps (Fig. 5). Their strengths of connections were similar in both methods, except for cerebellum and superior temporal gyrus that were more strongly connected in TMS/PET. There were several areas that were connected to the SMA in the electrophysiological map. They include left prefrontal areas, right-sided insula, visual areas, and temporal regions. Additionally, several brain areas that were seen on the electrophysiological map appear to be a result of direct stimulation (especially at 125% rMT intensity) (see Table 3). We also found brain regions seen only in MACM, including bilateral inferior frontal gyrii and inferior parietal lobules, the left insula, and the right thalamus.

Comparison of behavioral profiles

We examined the behavioral domains ascribed to the brain regions included in the electrophysiological and the MACM maps. For each map, we included all the regions found to be significant in the previous analysis (Table 3 for TMS/PET; Table 4 for MACM). The behavioral domain attributes inferred from experimental design are tabulated for each study entered into the BrainMap database. While the BD information is derived from the database, the regions were input from the electrophysiological mapping derived from TMS/PET and the MACM derived from the database. Fig. 6 demonstrates the results of this analysis. Collectively, the brain areas identified by TMS/PET and MACM were seen to be active across several BD. Not surprisingly, action execution had the highest representation in the two datasets. Both TMS/PET and MACM networks were engaged in most of the behavioral sub-domains of action. However, both TMS/PET and MACM networks were also engaged during cognitive and perceptual processes. While MACM regions were invoked under several sub-domains of cognition and perception, TMS/PET network is engaged during a sub-set of these behaviors that have a strong motor component such as language, music, somesthesis, motion, and shape perception. MACM regions appear to be engaged during emotion and interoceptual processes as well.

Domain-specific meta-analytic connectivity

We once again confirmed that the seed location was indeed located within the SMA for each of the domain specific MACM maps. The average reported Talairach locations of SMA in the experiments were at x, y, z co-ordinates of (5, −6, 51) for action; (5, −5, 51) for perception; (5, −5, 52) for cognition; and (5, −5, 51) for emotion and interoception. The regions that co-varied with the SMA for the functional domains of action, perception, cognition, and emotion and interoception domain are listed in Fig. 7. The right cerebellum was found to co-activate with R-SMA across all the behavioral domains (Fig. 7). Left insula (BA 13) co-varied with SMA in the behavioral domains of action, cognition and perception, and right inferior frontal gyrus (BA 44) co-varied with the SMA in the behavioral domains of action, cognition, and emotion and interoception.

We also identified several brain regions that were common across two functional domains (Fig. 7). The R-SMA was found to strongly covary bilaterally with dorsal pre-motor areas (BA 6) and basal ganglia across the behavioral domains of action and cognition. In addition, left sided superior parietal lobule (SPL; BA 7), IPL (BA 40), precuneus (BA 7), primary motor cortex, superior temporal gyrus, and cerebellum (Fig. 7) co-activated with R-SMA under these domains. The right inferior frontal gyrus (BA 9) was also found to co-activate with the R-SMA during performance of action and cognitive tasks. Bilateral thalami and the right insula (BA 13) were found to co-vary with the SMA under the domains of action and perception. The left occipital cortex (BA 18) was seen to be co-active in the cognitive and emotion and interoceptive domains (Fig. 7).

Further, several brain regions were observed to be related with SMA activity in the context of a single behavioral domain (Fig. 7). Only action tasks resulted in concurrent activity in right-sided primary motor cortex (BA 4), inferior parietal lobule (BA 40), superior parietal lobule (BA 7), and bilateral post central gyri (BA 3/2). Under the cognitive domain, left sided middle and inferior frontal gyri (BA 9, BA 46, BA 44), middle temporal gyrus (BA 22) and transverse temporal gyrus (BA 42) co-activated with R-SMA. Tasks related to perception resulted in co-activation of the right postcentral gyrus (BA 40) and cingulate gyrus (BA 24) along with SMA.

The volumes of significant activations in the action MACM and TMS/PET showed significant overlap, with a Pearson correlation of 0.32 ($p<0.0001$). Correlations between the cognition MACM and TMS/PET was 0.28 ($p<0.0001$), between perception MACM and

TMS/PET was 0.27 ($p<0.0001$), and between emotion/interoception MACM and TMS/PET was 0.13 ($p<0.001$).

MACM of the left SMA

The MACM of the left SMA was remarkably similar to that of the right SMA. The cross correlation (Pearson) was high with $r=0.79$ ($p<0.0001$). Fig. 8 demonstrates this overlap where the right SMA MACM is shown in red, the MACM of the left SMA in green, and the overlap between the two maps in yellow. The left SMA MACM correlated with TMS/PET with a $r=0.4$ ($p<0.0001$), very similar to that of the right SMA MACM. This indicates that we can indeed generalize about connections of SMA.

Discussion

Brain regions can be anatomically and functionally categorized by ascertaining other regions that they are connected to (Crick and Jones, 1993). We examined this concept in the human SMA using electrophysiologic connectivity mapping by TMS/PET and functional connectivity with MACM. We successfully mapped the electrophysiological connectivity of SMA, and demonstrated that it was strongly connected to several bilateral motor regions in the frontal lobe, especially along the medial bank. We also identified that SMA was connected to primary and secondary sensory areas in the parietal lobe, prefrontal areas, insula, temporal cortex, and cerebellum. The functional connectivity map of SMA derived by MACM demonstrated a similar connectivity map, with a significant spatial concordance between the two maps. Behavioral profiling of the two connectivity maps demonstrated that these networks were also engaged in cognitive and perceptual processes, with MACM demonstrating a broader behavioral profile, while the electrophysiological map representation was more limited. MACM of individual behavioral domains also confirmed that SMA and its connected regions are invoked during a broad range of behaviors. Collectively, these data clearly reveal that the SMA is predominantly a part of the motor system, and is invoked during action. Additionally, the behavioral domain analysis of both electrophysiological and functional connectivity maps indicated that the SMA is also a component of cognitive, and perceptive networks. Finally, we demonstrate that the functional connectivity of the left SMA was very similar to the functional connectivity of the right SMA and that the findings from this study can be generalized.

In the following sections, we will overview the TMS/PET method of mapping electrophysiological connectivity, and the brain regions connected with the human SMA as identified by TMS/PET. Next, in order to examine the validity of these brain areas connected with the SMA, we will compare these connections to that derived from tract tracing in non-human primates. We will then examine the functional connectivity of SMA as identified by MACM, the behavioral profiles of the connected regions, and discuss the advantages of combining the two methods to study connectivity. Next, we will explore the potential roles that the SMA plays in human behavior under the broad headings of action, cognition, and perception. Finally, we will address some limitations of TMS/PET and MACM, and future directions.

Electrophysiologic connectivity of SMA

TMS combined with concurrent PET scanning provided a method of obtaining human intra-cerebral connectivity data in a "task-independent" manner. We identified SMA using a probabilistic strategy and successfully stimulated SMA. Even though SMA extends more dorsally, and the TMS E-field is stronger at the surface, we found that the peak response to TMS was located deeper in the sulcus ($z=50$, see Fig. 2). This observation is consistent with our previous findings in M1 (Fox et al., 2004, 2006) and supports the cortical column cosine principle (Fox et al., 2004). In addition, the stimulated region of SMA overlapped with the physiological location of SMA observed during finger tapping (Fig. 2), a finding also consistent with our previous results in M1 (Fox et al., 2004). Previously, we (Fox et al., 2004) have demonstrated that the depths of activation in M1 resulting from finger tapping and TMS co-vary significantly ($r=0.93$), indicating that both conditions elicited activation in the same cortical region. Therefore we are confident that we have successfully identified and stimulated the right SMA in this study and chose the peak location of SMA response to TMS as the seed for correlation and MACM analyses.

However, SMA is a large region with complex geometry and the selected seed volume could not encompass all of the right SMA. Parts of SMA are outside the dorsal and posterior margins of the seed volume (Picard and Strick, 2001), and parts of cingulate gyrus could lie within the seed volume. To further verify that the electrophysiological and functional connectivity maps reported here are indeed representative of SMA connectivity, we ran two additional MACM analyses where the seed volume was centered at a higher z (to include more of SMA), or had a smaller extent (to exclude cingulate gyrus). We examined the degree of spatial, and behavioral profile overlap between these MACMs and the SMA MACM reported in this study. We found that the spatial overlap between the dorsal SMA MACM and the SMA MACM was excellent with a Pearson correlation of 0.84 ($p<0.0001$). The smaller SMA MACM had a correlation of 0.80 ($p<0.0001$). The behavioral profiles of the three MACMs overlapped extensively as well. Therefore, we are confident that the connectivity maps reported here truly represent the electrophysiological and functional connectivity of the human SMA.

The CBF response in the SMA was successfully modulated parametrically with increasing TMS intensities (Table 2), which in turn propagated to connected areas. The brain areas closely connected to the SMA responded to increasing TMS intensities in a similar manner. This technique not only confirms synaptic viability (as action potential successfully propagated transynaptically to remote brain areas), it also can help assign direction of propagation of action potential (anterograde or retrograde). Remote downstream brain areas (such as M1, basal ganglion, cerebellum) were most likely activated from anterograde propagation of action potential, while activations in nearby regions, parietal regions, and prefrontal cortex may be a result of retrograde conduction of action potentials from the SMA. This strategy helped identify brain regions belonging to the motor, perceptual, and cognitive networks to be electrophysiologically connected with the SMA (Table 3, Fig. 3). Over all the right-sided human SMA is connected extensively along the medial aspects of frontal lobe including pre-SMA, supplementary eye field, and primary leg motor cortex. We interpret these to be the result of direct propagation of electrical activity from the SMA to adjacent areas or direct stimulation of these regions at 125% rMT. More remote frontal lobe connections of SMA were noted to bilateral primary motor cortices, dorsal and ventral pre-motor regions. We infer that these connections are seen due to the trans-synaptic propagation of electrical activity. Similar distant connections of SMA to bilateral primary sensory areas in the parietal lobe, insula, basal ganglia, thalami and cerebellum were also demonstrated. Prefrontal cortex (BA 9 and BA 10) and parietal areas (BA 5 and BA 7) may have been activated via retrograde propagation of action potentials from the SMA. In order to examine the validity of brain areas identified by TMS/PET to be connected with the SMA, we compared the electrophysiological connectivity map to that derived from tract tracing in non-human primates. Studies of motor regions in animals allow for a relatively easy comparison with homologous regions in humans. There exists a wealth of invasive tract tracing connectivity data relating to these regions in primates. This literature spans several decades and is therefore heterogeneous in methodology, anatomic nomenclature, and the animal model used (Akkal et al., 2007; Geyer et al., 2000; and Jurgens, 1984; Kunzle, 1978; Luppino et

al., 1993; McGuire et al., 1991; Rizzolatti et al., 1998). Regions homologous with the human SMA in the animal have been well delineated. The SMA—as defined by cytoarchitectonic criteria in primates—area 6aα of Vogt (Vogt and Vogt, 1919) or F3 of Matelli (Matelli et al., 1985; 1991) corresponds to the SMA proper in humans.

Comparison of TMS/PET connectivity map with anatomical connectivity of the macaque SMA

Of the vast number of tract tracing studies, we identified four studies that were directly relevant to the present study. These studies examined the connectivity of primate area 6aα (Vogt and Vogt, 1919) or F3 (Matelli et al., 1985; 1991), to the rest of the brain in *Macaca fascicularis* (Kunzle, 1978; McGuire et al., 1991; Rizzolatti et al., 1998) and *Saimiri sciureus* (Jurgens, 1984). In these studies wheat germ agglutinin tagged with horseradish peroxidase or radiotracers (tritiated amino-acids) was injected into the SMA, and the brain sectioned after an interval. To facilitate comparison with humans, the results of these studies that were converted to equivalent Brodmann area sub-categorization (Vogt and Vogt, 1919) was utilized only when essential to describe functional roles. Given that cortico-cortical connections are generally reciprocal (Jurgens, 1984; McGuire et al., 1991) and no significant differences exist—in macaques—between the right vs. the left SMA connectivity (McGuire et al., 1991, see also Fig. 8 for humans), results are summarized across hemisphere and across anterograde and retrograde tracers.

There were striking similarities between the cortical connectivity of the human SMA derived from TMS/PET and the invasive tracer-derived measures of connectivity. Across all the invasive tract-tracing studies included here, the SMA was extensively connected with the motor cortex (BA 4), the premotor cortex (BA 6 and BA 44), dorsomedial prefrontal cortex (BA 9), cingulate cortex (BA 24), and post central gyrus (BA 1 and BA 2), BA 5, and BA 7 in the parietal lobe. The connectivity of SMA with nearly pre-SMA, supplementary eye field, and premotor cortex were also noted, and supports the notion that cortical regions project to their geographic neighbors (Hellwig, 2000; Young et al., 1995) presumably via U fibers, and strong connection between SMA and M1-leg is also concordant with this view. Additional remote connections were also noted with the superior temporal lobe, the frontal operculum, insula, parietal operculum, posterior cingulate cortex, the basal ganglia (putamen and caudate nucleus), claustrum, and other sub-cortical nuclei. Connection of SMA to various thalamic nuclei, substantia nigra, red nucleus, and other sub-cortical structures were also observed in these studies.

We did observe some differences between the connectivity mapping by TMS/PET and the tract tracing, mainly in regards to the cerebellum, and the subcortical structures. The first difference was that the cerebellum was found to co-activate with the SMA in the TMS/PET study but connections between these two regions have not been reported in the primate literature. This may be consequent to the time that it takes for axonal transport to the cerebellum (Wiesendanger and Weisendanger, 1985b). Another reason for this may be that the connection between SMA and cerebellum is indirect and not detected by tract tracing methods. It has been shown that the pyramidal cells in layer 5 of SMA connect to the cerebellum (vermis, pyramis and centralis) through the pontine nuclei and inferior cerebellar peduncle (Glickstein and Doron, 2008). Similarly the cerebellar nuclei project indirectly to the frontal lobe via the venteroposterolateral (VPL) and venterolateral (VL) nuclei of thalamus (Sommer, 2003). These fibers preferentially connect cerebellum to M1 and PMd, and less to the SMA and likely reflect the substrates of the cerebellar audit of sensorimotor processing, modulation of axial tone, and motor co-ordination. While these indirect connections can be mapped by TMS/PET, tract tracing cannot identify them. Another distinction between tract tracing and TMS/PET results was the weak correlation of SMA activity with the basal ganglia and thalamus seen in TMS/PET while animal tract tracing studies have demonstrated strong connections between these regions. These connections while evident by TMS/PET method, did not reach significance due to volume $<150\ mm^3$ (Table 3) in the correlation analysis. One possible explanation for this finding is discussed in detail later under the section Potential limitations of TMS/PET connectivity mapping. A third difference between the two methods was noted in that the connections of SMA to sub-cortical structures such as the substantia nigra, and the red nucleus reported by tract tracing were not observed in the TMS/PET study. The poor spatial resolution of PET (in the order of 8–10 mm) in large part limited the delineation of the small suborbital structures such as substantia nigra, and red nucleus in the current TMS/PET study. We demonstrate that the cortical connectivity of the SMA identified by electrophysiological mapping correspond strongly with maps obtained by tract tracing in primates. The dissimilarities between the two methods appear to arise from methodological differences (inability to detect indirect connections by tract tracing, and poor spatial resolution of PET imaging), and were limited to subcortical and cerebellar connections of the SMA.

Functional connectivity of SMA

Pooling of brain regions that were co-activated with SMA across all behavioral domains resulted in a composite task dependent functional connectivity map (Fig. 4). In this study, we aimed to outline the functional connectivity of SMA, by examining the brain regions that were co-activated with SMA. The entire BrainMap database was searched for studies that reported activation within the seed volume. We then tabulated the co-ordinates of other brain regions that were reported to be active in these studies. In this manner, MACM is analogous to the TMS/PET study. We did not include deactivations in our analysis as deactivations pooled across several conditional contrast studies have been shown to be mostly components of the default mode network (Laird et al., 2009). In this particular analysis, pooling the functional studies across behavioral domains did not cancel out the behavioral influence, but rather enhanced the behavioral domains that the seed region was significantly involved in. Thus, since we only identified brain regions that always co-activated with the SMA, we expected to isolate mainly the behavioral domains in which the SMA was active.

Activation likelihood estimation (ALE) is a co-ordinate based meta-analysis of imaging studies that improves the identification of brain areas that are involved in one specific task or behavior (Laird et al., 2005; Turkeltaub et al., 2002), but does not necessarily inform on all the behaviors that a brain region could be involved in. In order to examine the role of one brain region (seed region), we performed MACM, which apprises on all the behaviors that a brain region was activated in. In addition, MACM provided information about which other brain areas were engaged during that behavior. In generating the domain specific MACMs, we sought to find the brain areas which are co-activated with the seed volume under a particular behavioral domain.

Functional connectivity of SMA (Table 4, Fig. 4) demonstrated that other motor areas in the frontal lobe such as the primary motor cortex, dorsal premotor cortex, and inferior frontal gyrus, as well as putamen and cerebellum co-activated with SMA during task performance, and indicated to the motor function of SMA. Additionally, co-activation of post central gyrus, superior and inferior parietal lobules, insula, superior temporal lobe, and thalamus, clearly point to the role of SMA in perception, perhaps driven by somatosensory and auditory input.

Comparison of electrophysiological and functional connectivity of the SMA

We observed a significant spatial correlation between the electrophysiological and functional connectivity maps. Several regions were commonly identified in both maps (Fig. 5). We found that the regions that were most strongly correlated with the SMA in the

electrophysiological map were also seen in the functional connectivity map, confirming the principle that brain regions that are "wired together fire together". There were several areas that were connected to the SMA in the electrophysiological map that were not observed in the overall functional map, including left prefrontal areas, right-sided insula, visual areas, and temporal regions. These regions were not as strongly correlating with the SMA indicating that their CBF response profile was less similar to that observed in the SMA, signifying that these connections could be more indirect (i.e. a few synapses removed). However, these areas co-activated with the SMA in the individual domain MACMs, once again signaling to the multi-domain nature of the electrophysiological connectivity. Additionally, several brain areas that were seen on the electrophysiological map appear to be a result of direct stimulation (especially at 125% rMT intensity) (see Table 3). We also found brain regions seen only in MACM, including bilateral inferior frontal gyri and inferior parietal lobules, the left insula, and the right thalamus. The experiments included in the BrainMap database represent a wide range of tasks, paradigms, various types of control tasks, and different levels of conditional contrasts and therefore, the co-activation pattern derived by MACM could identify unrelated brain regions to be co-activating with the SMA, in part as a result of a different experimental paradigm or an inappropriate contrast condition. On the other hand, we cannot rule out the possibility that these functional connections are valid, and it is the action potential generated at the SMA by TMS, that failed to propagate across several synapses. Lastly, brain regions activated via feedback or relay processes, transmitted through cascades of several intermediates or via cortical–subcortical loops (Eickhoff et al., 2009b; Grefkes et al., 2008a) can appear to be functionally connected to a brain region. Such propagation of neuronal activity cannot be detected by TMS/PET. The degree of correlation between the two maps could be readily improved by increasing the number of subjects studied. Additionally, modifying the TMS parameters to reduce spread of stimulation to the surrounding regions and drive the remote connected areas more effectively, for example using TMS rate as a parametric to drive the SMA, could also improve the spatial correlation between the two maps.

We examined the behavioral domains ascribed to the brain regions included in the electrophysiological and the MACM maps (Fig. 6). Collectively, the brain areas identified by these two maps were active across several BD. The two maps had strikingly similar BD profile for all subdomains of action. Interestingly, only the subdomains with the highest z scores in the MACM map were the only sub-domains observed in the electrophysiological map. These subdomains were language, music, somesthesis, motion, and shape perception, all of which have a strong motor component. This may be another indication that the strongest activations are in areas that are closely connected anatomically.

Domain-specific meta-analytic connectivity

When the co-activation patterns were isolated for each behavioral domain, complex patterns of connectivity emerged. We observed that the SMA was connected to several brain areas that were themselves multimodal as well as brain areas that were less so (Fig. 7). For example, regions such as cerebellum, insula, and IFG appear to be co-activated with the SMA across the behavioral domains studied here: action, perception, cognition as well as emotion and interoception. By this analysis, several areas in the parietal lobe were found to be co-activated with the SMA during action, as well as cognition. Similarly, thalamus, basal ganglion, and dorsal premotor areas appear to have multimodal functions. However, we also identified several brain areas that are co-activating with the SMA uniquely under individual behavioral domains. For example, primary motor and sensory cortices co-vary with the SMA only under the behavioral domain of action. Similarly, left sided prefrontal and temporal areas co-varied with the SMA only while performing cognitive tasks, and parietal and cingulate cortices were co-activating with the SMA only during performance of tasks involving perception. The degree of spatial correlation of the domain specific MACMs with the electrophysiological map was directly indicative of the relative significance of the behavioral domains, with action MACM having the highest correlation, and the emotion and interoception MACM correlating the least.

Advantages of multimodal connectivity mapping

In this study, multimodal connectivity mapping was used to develop a comprehensive connectivity map of the human SMA. While the electrophysiological connectivity mapping identified brain areas synaptically connected with the SMA, functional connectivity mapping delineated the functional role of these regions. More significantly, the electrophysiological connectivity mapping confirmed the multi-domain role of the SMA. The brain regions identified to be part of the motor system, the perceptual system, and cognitive systems were closely connected to the SMA. The electrophysiological map in most part reflected the degree of functional coupling between areas. The brain areas most strongly co-varying with SMA (higher r) in the electrophysiological map had the greatest functional significance (higher ALE score). Amidst the spectrum of available techniques of connectivity mapping, with DTI at one end providing sparse anatomical connectivity, and functional connectivity mapping at the other end yielding an exaggerated connectivity, electrophysiological connectivity mapping with TMS/PET is an optimal intermediary. Connectivity map derived from TMS/PET provides greater detail on the anatomical connectivity highlighting synaptic viability and direction of flow, and isolates only the relevant functional connections. However, we found an instance where the functional connectivity map aided in the interpretation of a weak anatomical connection for example between the SMA and the basal ganglion, that was found to be strong in the functional connectivity map. Such a finding is consistent with previous observations that a weak anatomical connection can still hold high functional significance (Friston, 2002; Grefkes et al., 2008b). Presently, no technique provides a connectivity map of a region in its entirety; therefore, combining multimodal connectivity mapping methods is critical towards generating comprehensive connectivity maps of brain regions.

Role of SMA in human behaviors

Action

In the current study, the connectivity of SMA to other regions in the motor network derived from MACM and TMS/PET reflects the brain regions that are connected with the SMA in the behavioral domain of action. Across the action/motor domain, SMA was primarily co-activated with other frontal lobe motor areas such as dorsal premotor and primary motor cortices, and parietal lobe regions including S1, SPL, IPL, and precuneus. In addition SMA was connected with insula, basal ganglia, thalami, and cerebellum. Most of these connections were demonstrated to be electrophysiological by TMS/PET. Covariance between SMA and PMd indicates to a dynamic interplay between these two executive areas in movement regulation, whether internally cued and over learned (SMA) or externally cued and novel (PMd), and may suggest to a synergistic organization of sequential motion in response to internal or external information (Tanji and Shima, 1996). SMA is thought to integrate the sensory information and transform it into a motor representation (Luppino and Rizzolatti, 2000) and/or produce a complementary set of motor commands (Dum and Strick, 2002). It is also suggested that SMA in concert with M1 may play a primary role in the control of posture and, in particular, in postural adjustments preceding voluntary movements (Luppino and Rizzolatti, 2000). Connections between the SMA and the basal ganglia likely facilitate the co-ordination of motor output as suggested by theories of basal ganglia function (DeLong, 1973, DeLong et al., 1986; Lehéricy et al., 2004). Thalamus is thought to then act as a filter for

low frequency tonic activity, while relaying high frequency phasic bursts originating from basal ganglion to motor areas (Sommer, 2003). Co-activation of cerebellum with SMA during action likely reflects the cerebellar audit of sensorimotor processing, modulation of axial tone, and motor co-ordination. Thus, SMA appears to be not only important for overall motor planning and execution (via its interaction with primary motor cortex), but for various finer levels of movement control (via its connection to thalamus, basal ganglia, cerebellum and spinal cord) (Jurgens, 1984). Lesions of SMA result in decreased volitional effort and akinetic mutism that clearly indicate to the important role SMA plays in action/execution. The SMA's interaction with several areas of the motor network indicates to the extensive role it may play from initiation of global motor plans to influence smaller aspects of the network such as spinal reflexes.

Perception

SMA's role in perception appears to be its next important function (20% of studies included in the domain independent MACM reporting SMA activation during perceptual task performance). SMA was found to be co-activating with the cingulate cortex, post central gyrus, insula, thalamus, putamen, cerebellum, and inferior frontal gyrus during performance of isolated perceptual tasks. Several of these connections were confirmed by TMS/PET. SMA was co-activated with these areas not only under the perceptual domain, but also when the co-activation pattern was limited to the behavioral domain of action only, with exclusion of all perceptual tasks included in the BrainMap database. Thus, SMA and several areas in the parietal lobe were found to be inter-connected during action and perception. Sensory information appears to reach SMA indirectly: via superior temporal sulcus for visual and auditory stimuli, BA 5, BA 7, and parietal operculum for somatosensory stimuli (Jurgens, 1984). SMA connections with the superior parietal lobule likely indicate pathways responsible for cross modal sensori-motor transformation and complex actions. Recently, a reduction in gray matter volumes in these very regions: SMA, SPL, and precuneus was demonstrated in patients with developmental dyslexia with impaired implicit motor learning (Menghini et al., 2008), indicating a close connection between these areas in motor, perceptual and cognitive domains. Connections of SMA with the IPL and the precuneus have been shown to be important in motor imagery (Hanakawa et al., 2003, Malouin et al., 2003, Ogiso et al., 2002). Connections of SMA with S1 indicate pathways for monitoring motor execution. As a whole, the SMA is intimately connected with the parietal spatial reference network. Connections with the insula reflect pathways essential for sensori-motor integration. These findings are consistent with the parieto-frontal circuits that are organized for optimal sensorimotor transformation (Rizzolatti et al., 1998). Further, the activation of SMA specifically under the behavioral domain of pain may indicate a protective mechanism in which motor plans for flight responses are rapidly generated.

Cognition

Approximately a third of the data of domain general MACM analysis were contributed by cognitive tasks, suggesting to the important role of SMA in cognition. Since many cognitive tasks include a motor component such as button press and overt speech, the co-activation of SMA could be due to the concomitant motor task. To rule out such a possibility, we examined the SMA co-activations in the experiments that were coded only under the cognitive domain. ALE analysis of the resulting data revealed that SMA continued to be co-activated during the performance of cognitive tasks. Different from the action and perceptual domains, the SMA was connected to cingulate cortex, several prefrontal areas (BA 44, BA 45, BA 46, BA 9), as well as temporal areas (BA 41 and BA 22) during performance of cognitive tasks. The SMA was also connected with motor and pre-motor areas, SPL, IPL, insula, thalamus, basal ganglia as well as the cerebellum. TMS/PET demonstrated that several of these areas were electrophysiologically connected with the SMA.

Brain areas such as $M1_{mouth}$, insula, inferior frontal gyrus (BA 44), middle frontal gyrus (BA 9 and BA 46), middle temporal gyrus (BA 22), as well as basal ganglia, and the cerebellum along with the SMA are components of the articulatory network (Guenther et al., 2006). In fact, the earliest reference to the SMA as a distinct area in humans, pointed to its role in vocalization (Foerster, 1936; Penfield and Welch, 1951). SMA along with M1, PMd, anterior cingulate cortex, IPL, basal ganglia, thalamus, cerebellum,and ventrolateral prefrontal cortex have been demonstrated to be involved in motor skill learning (Doyon et al., 2009). SMA, by being a part of the cortico-striatal as well as cortico-cerebellar networks, has been shown to be important not only in the early phases of learning, but also to be important in the execution and retention of motor learning and motor adaptation (Debas et al., 2010; Doyon et al., 2003, 2009). We demonstrate here that indeed all these regions are interconnected with the SMA in the cognitive domain.

Connections of the right SMA were seen with ipsilateral prefrontal regions (BA 9 and BA 45) as well. These projections may represent feedback loops to the cortical substrates for the cognitive control of action (Lau et al., 2004). The extensive connectivity of the SMA with the frontal lobes the mesial motor complex, primary and premotor cortex, and dorsal prefrontal cortex in the context of cognition lends credence to the view that the network involved in action selection and modulation extends beyond the medial fronto-limbic region to include much of the frontal lobe (Passingham, 1993). As far as semantic and lexical processing are concerned, SMA co-activation is consistent with the observation that cognition, especially object concept is not only represented in the language/cognitive network, but is also grounded in the sensory (sensory features such as form, motion, color) and the motor (motor properties such as how to use) systems as well (Martin, 2007).

Potential limitations of TMS/PET connectivity mapping

An important distinction between tract tracing and TMS/PET was the weak correlation of SMA activity with the basal ganglia and thalamus seen in TMS/PET. These connections while evident by TMS/PET method, did not reach significance due to volume $<150\ mm^3$ (Table 3) in the correlation analysis. However, lentiform nucleus and thalamus bilaterally showed significant activation in conditional contrasts of all TMS intensities vs. sham. It is possible that the communication between SMA and the sub-cortical regions appear to be "on" during all TMS conditions, and do not linearly co-vary with intensity of SMA activity. We therefore examined the activation of SMA, basal ganglia, and thalamus at each intensity level used for TMS stimulation. The z-scores of activation at SMA were 2.52, 2.89, and 2.7 for 75% rMT vs. sham, 100% rMT vs. sham and 125% rMT vs. sham respectively (Table 2). For the same conditions the z-scores at lentiform nucleus were 2.5, 2.8 and 2.56 respectively. A similar response pattern was observed in thalamus as well. So while SMA activity increased with TMS intensity, reaching a plateau at 125% rMT, the basal ganglion and thalamic activities were independent of TMS intensity. Such a phenomenon would explain the weak covariance of basal ganglion and thalamus with the SMA seen in TMS/PET. Therefore, one of the drawbacks of TMS/PET mapping can be the inability to identify brain regions that do not linearly co-vary with the stimulated area. In such instances, functional connectivity mapping can be used to derive the strength of connections.

Another limitation that may restrict the use of TMS enhanced connectivity analysis is accurate targeting. Our aiming strategy was based on population data unrelated to the participants and not on individual functional imaging. Despite this limitation, as well as individual anatomic variability and inaccuracies inherent in spatial normalization, a regional activation was induced by TMS within the SMA (Fig. 2). Such a strategy is effective in targeting areas with consistent activation in a

population, for example motor regions. We have recently developed an individualized aiming strategy that uses functional localization of the target in each participant's brain, target identification relative to surface landmarks, and stereotactic software for optimized robotic positioning of the TMS coil, for participant-specific targeting (Narayana et al., 2009; Rábago et al., 2009).

Use of intensity to parametrically drive SMA was an effective way of identifying brain areas co-varying with the SMA. However, we found that at the highest intensity used in this study, several neighboring cortical areas were stimulated directly, adding noise to the connectivity map. Since there are no simple behavioral measures of SMA activation, the intensities of TMS used in this study were based on the resting motor threshold, derived from stimulating a different motor area, the primary motor cortex. We found that the intensity that was too weak to produce any evoke potentials (75% rMT), resulted in a significant activation in the SMA, indicating that neurons in the SMA have a much lower stimulation threshold. One way to overcome this problem, is to assess the optimal stimulation intensities for nonprimary motor cortex brain areas directly as E-fields (V/m). Another solution would be to use TMS rate to parametrically manipulate the activity in a brain region (Salinas F, personal communication).

Another possible limitation of TMS/PET is the inability to target deeper cortical areas and sub-cortical brain areas. Using the conventional TMS coils (such as the B-shape coil or the figure-8 coil) brain areas that are about 30–40 mm from the scalp surface on its convexity can be stimulated. Connectivity mapping of deeper brain structures using such TMS coils is not possible at the present time. Newer coils (H coils) that are currently being developed and tested (Zangen et al., 2005) can overcome this drawback in the future.

Potential limitations of MACM

The experiments included in the BrainMap database represent a broad range of tasks, and therefore, the co-activation pattern derived by MACM could identify brain regions not functionally connected with SMA. We set high thresholds for statistical significance and cluster size in the ALE analysis in order to overcome this problem. Therefore, we are confident that only brain areas that co-activated with SMA consistently across several studies were included in our analysis.

One potential drawback of MACM is the difference in the number of reported activations in each of the BD coded in the BrainMap. However, we corrected for these differences, and still found significant involvement of SMA and its connected regions in cognition and perception. Even though cognitive experiments far outweigh the number of action experiments, the most significant BD was action in this analysis, indicating that the SMA functional connectivity map identified by the MACM was not unduly influenced by the domain distribution pattern of BrainMap. The coding and data analyses paradigms in the BrainMap project are being continually optimized to overcome these limitations (Laird et al., 2011b). Use of reverse inference approach is another way to alleviate this problem (Yarkoni et al., 2011).

An important aspect of functional imaging is that it is task based, and involves several behavioral domains, therefore it is difficult to isolate brain areas active when engaged in a particular behavioral domain or sub-domain. Indeed, the behavior domain profiling of each domain specific MACM indicated that we could not isolate the domains completely. However, the action domain MACM had most representation of action sub-domains, while cognition MACM had a much greater representation in its sub-domain, and the perception MACM was also similarly weighted by its sub-domains. Thus, while we cannot isolate brain areas into individual behavioral domains, it is certainly possible to bias the data to the domain of interest.

Summary

The electrophysiological and functional SMA connectivity map generated here by multimodal imaging corroborates several system level theories—the existence of multiple motor areas on the medial aspect of the hemisphere, the widespread neural substrates involved in action regulation, and the role of the SMA in motor behavior, somatic orientation and posture, sensory motor integration, as well as speech and motor skill learning. These maps include several components of motor, perceptual, and cognitive networks. Importantly, the cortical connectivity of the SMA identified by electrophysiological mapping concurred with the maps obtained by tract tracing in primates. The next step in this research is to apply the more rigorous modeling techniques such as direct causal modeling or structural equation modeling to model the SMA connectivity in different behavioral domains. Such models can be used to examine changes in a specific domain following interventions such as treatment or skilled training. The availability of such data in humans will facilitate the development of computational networks to describe plasticity in human neural interactions following treatment and/or training.

Acknowledgments

We thank Betty Heyl and Sergo Leal for assistance with PET data acquisition; Drs. Yulin Pu and Jia-Hong Gao for assistance with MRI data acquisition; and Tanya Taylor for assistance in BrainMap meta-analysis. This work was funded by grants from the National Institute of Mental Health (RO1-MH60246 and R01-MH074457-01A1 awarded to P.T. Fox), and the National Institute of Deafness and Communication Disorders (R21-DC009467-01A1 to S. Narayana).

References

Akkal, D., Dum, R.P., Strick, P.L., 2007. Supplementary motor area and presupplementary motor area: targets of basal ganglia and cerebellar output. J. Neurosci. 27 (40), 10659–10673.

Behrens, T.E., Johansen-Berg, H., 2005. Relating connectional architecture to grey matter function using diffusion imaging. Philos. Trans. R. Soc. Lond. B Biol. Sci. 360 (1457), 903–911.

Biswal, B., Yetkin, F.Z., Haughton, V.M., Hyde, J.S., 1995. Functional connectivity in the motor cortex of the resting human brain using echo-planar MRI. Magn. Reson. Med. 34 (4), 537–541.

Brodmann, K., 1905. Beitraege zur histologischen Lokalisation der Grosshirnrinde. III Mitteilung. Die Rindenfelder der niederen Affen. J. Psychol. Neurol. (Lzp.) 4, 177–226.

Catalan, M.J., Honda, M., Weeks, R.A., Cohen, L.G., Hallett, M., 1998. The functional neuroanatomy of simple and complex sequential finger movements: a PET study. Brain 121 (Pt 2), 253–264.

Cauda, F., Cavanna, A.E., D'agata, F., Sacco, K., Duca, S., Geminiani, G.C., 2011. Functional connectivity and coactivation of the nucleus accumbens: a combined functional connectivity and structure-based meta-analysis. J. Cogn. Neurosci. 23 (10), 2864–2877.

Chouinard, P.A., Van Der Werf, Y.D., Leonard, G., Paus, T., 2003. Modulating neural networks with transcranial magnetic stimulation applied over the dorsal premotor and primary motor cortices. J. Neurophysiol. 90 (2), 1071–1083.

Chung, G.H., Han, Y.M., Jeong, S.H., Jack Jr., C.R., 2005. Functional heterogeneity of the supplementary motor area. AJNR Am. J. Neuroradiol. 26 (7), 1819–1823.

Colebatch, J.G., Deiber, M.P., Passingham, R.E., Friston, K.J., Frackowiak, R.S., 1991. Regional cerebral blood flow during voluntary arm and hand movements in human subjects. J. Neurophysiol. 65 (6), 1392–1401.

Crick, F., Jones, E., 1993. Backwardness of human neuroanatomy. Nature 361 (6408), 109–110.

Debas, K., Carrier, J., Orban, P., Barakat, M., Lungu, O., Vandewalle, G., Hadj Tahar, A., Bellec, P., Karni, A., Ungerleider, L.G., Benali, H., Doyon, J., 2010. Brain plasticity related to the consolidation of motor sequence learning and motor adaptation. Proc. Natl. Acad. Sci. U.S.A. 107 (41), 17839–17844.

DeLong, M.R., 1973. Putamen: activity of single units during slow and rapid arm movements. Science 179 (79), 1240–1242.

DeLong, M.R., Alexander, G.E., Mitchell, S.J., Richardson, R.T., 1986. The contribution of basal ganglia to limb control. Prog. Brain Res. 64, 161–174.

Doyon, J., Benali, H., 2005. Reorganization and plasticity in the adult brain during learning of motor skills. Curr. Opin. Neurobiol. 15 (2), 161–167.

Doyon, J., Penhune, V., Ungerleider, L.G., 2003. Distinct contribution of the cortico-striatal and cortico-cerebellar systems to motor skill learning. Neuropsychologia 41 (3), 252–262.

Doyon, J., Bellec, P., Amsel, R., Penhune, V., Monchi, O., Carrier, J., Lehéricy, S., Benali, H., 2009. Contribution of the basal ganglia and the functionally related brain structures to motor learning. Behav. Brain Res. 199 (1), 61–75.
Dum, R.P., Strick, P.L., 2002. Motor areas in the frontal lobe of the primate. Physiol. Behav. 77 (4–5), 677–682.
Eickhoff, S.B., Paus, T., Caspers, S., Grosbras, M.H., Evans, A.C., Zilles, K., Amunts, K., 2007. Assignment of functional activations to probabilistic cytoarchitectonic areas revisited. Neuroimage 36 (3), 511–521.
Eickhoff, S.B., Heim, S., Zilles, K., Amunts, K., 2009a. A systems perspective on the effective connectivity of overt speech production. Philos. Transact. A Math. Phys. Eng. Sci. 367, 2399–2421.
Eickhoff, S.B., Laird, A.R., Grefkes, C., Wang, L.E., Zilles, K., Fox, P.T., 2009b. Coordinate-based activation likelihood estimation meta-analysis of neuroimaging data: a random-effects approach based on empirical estimates of spatial uncertainty. Hum. Brain Mapp. 30 (9), 2907–2926.
Ferrarelli, F., Haraldsson, H.M., Barnhart, T.E., Roberts, A.D., Oakes, T.R., Massimini, M., Stone, C.K., Kalin, N.H., Tononi, G., 2004. A [17F]-fluoromethane PET/TMS study of effective connectivity. Brain Res. Bull. 64 (2), 103–113.
Fiez, J.A., Petersen, S.E., 1998. Neuroimaging studies of word reading. Proc. Natl. Acad. Sci. U.S.A. 95 (3), 914–921.
Foerster, O., 1936. The motor cortex in man in light of Hughlings Jackson's doctrines. Brain 59 (2), 10–159.
Fox, M.D., Raichle, M.E., 2007. Spontaneous fluctuations in brain activity observed with functional magnetic resonance imaging. Nat. Rev. Neurosci. 8 (9), 700–711.
Fox, P.T., Mintun, M.A., Raichle, M.E., Herscovitch, P., 1984. Noninvasive approach to quantitative functional brain mapping with H2(15)O and positron emission tomography. J. Cereb. Blood Flow Metab. 4 (3), 329–333.
Fox, P., Ingham, R., George, M.S., Mayberg, H., Ingham, J., Roby, J., Martin, C., Jerabek, P., 1997. Imaging human intra-cerebral connectivity by PET during TMS. Neuroreport 8 (12), 2787–2791.
Fox, P.T., Ingham, R.J., Ingham, J.C., Zamarripa, F., Xiong, J.H., Lancaster, J.L., 2000. Brain correlates of stuttering and syllable production. A PET performance-correlation analysis. Brain 123 (10), 1985–2004.
Fox, P.T., Narayana, S., Tandon, N., Sandoval, H., Fox, S.P., Kochunov, P., Lancaster, J.L., 2004. A column-based model of electric field excitation of cerebral cortex. Hum. Brain Mapp. 22, 1–16.
Fox, P.T., Narayana, S., Tandon, N., Fox, S.P., Sandoval, H., Kochunov, P., Capaday, C., Lancaster, J.L., 2006. Intensity modulation of TMS-induced cortical excitation: primary motor cortex. Hum. Brain Mapp. 27 (6), 478–487.
Friston, K., 2002. Functional integration and inference in the brain. Prog. Neurobiol. 68, 113–143.
Friston, K.J., Frith, C.D., Liddle, P.F., Frackowiak, R.S., 1993. Functional connectivity: the principal-component analysis of large (PET) data sets. J. Cereb. Blood Flow Metab. 13 (1), 5–14.
Gelnar, P.A., Krauss, B.R., Sheehe, P.R., Szeverenyi, N.M., Apkarian, A.V., 1999. A comparative fMRI study of cortical representations for thermal painful, vibrotactile, and motor performance tasks. Neuroimage 10 (4), 460–482.
Gerardin, E., Sirigu, A., Lehéricy, S., Poline, J.B., Gaymard, B., Marsault, C., Agid, Y., Le Bihan, D., 2000. Partially overlapping neural networks for real and imagined hand movements. Cereb. Cortex 10 (11), 1093–1104.
Geyer, S., Matelli, M., Luppino, G., Zilles, K., 2000. Functional neuroanatomy of the primate isocortical motor system. Anat. Embryol. (Berl) 202 (6), 443–474.
Glickstein, M., Doron, K., 2008. Cerebellum: connections and functions. Cerebellum 7 (4), 589–594.
Goerres, G.W., Samuel, M., Jenkins, I.H., Brooks, D.J., 1998. Cerebral control of unimanual and bimanual movements: an H2(15)O PET study. Neuroreport 9 (16), 3631–3638.
Grahn, J.A., Brett, M., 2007. Rhythm and beat perception in the motor areas of the brain. J. Cogn. Neurosci. 19 (5), 893–906.
Grefkes, C., Nowak, D.A., Eickhoff, S.B., Dafotakis, M., Kust, J., Karbe, H., Fink, G.R., 2008a. Cortical connectivity after subcortical stroke assessed with functional magnetic resonance imaging. Ann. Neurol. 63, 236–246.
Grefkes, C., Eickhoff, S.B., Nowak, D.A., Dafotakis, M., Fink, G.R., 2008b. Dynamic intra- and interhemispheric interactions during unilateral and bilateral hand movements assessed with fMRI and DCM. Neuroimage 41, 1382–1394.
Guenther, F.H., Ghosh, S.S., Tourville, J.A., 2006. Neural modeling and imaging of the cortical interactions underlying syllable production. Brain Lang. 96 (3), 280–301.
Hanakawa, T., Immisch, I., Toma, K., Dimyan, M.A., Van Gelderen, P., Hallett, M., 2003. Functional properties of brain areas associated with motor execution and imagery. J. Neurophysiol. 89 (2), 989–1002.
Haslinger, B., Erhard, P., Weilke, F., Ceballos-Baumann, A.O., Bartenstein, P., Gräfin von Einsiedel, H., Schwaiger, M., Conrad, B., Boecker, H., 2002. The role of lateral premotor-cerebellar-parietal circuits in motor sequence control: a parametric fMRI study. Brain Res. Cogn. Brain Res. 13 (2), 159–168.
Hellwig, B., 2000. A quantitative analysis of the local connectivity between pyramidal neurons in layers 2/3 of the rat visual cortex. Biol. Cybern. 82 (2), 111–121.
Ilmoniemi, R.J., Virtanen, J., Ruohonen, J., Karhu, J., Aronen, H.J., Näätänen, R., Katila, T., 1997. Neuronal responses to magnetic stimulation reveal cortical reactivity and connectivity. Neuroreport 10 (8(16)), 3537–3540.
Indovina, I., Sanes, J.N., 2001. Combined visual attention and finger movement effects on human brain representations. Exp. Brain Res. 140 (3), 265–279.
Jäncke, L., Peters, M., Himmelbach, M., Nösselt, T., Shah, J., Steinmetz, H., 2000. fMRI study of bimanual coordination. Neuropsychologia 38 (2), 164–174.
Johansen-Berg, H., Rushworth, M.F., 2009. Using diffusion imaging to study human connectional anatomy. Annu. Rev. Neurosci. 32, 75–94.
Joliot, M., Papathanassiou, D., Mellet, E., Quinton, O., Mazoyer, N., Courtheoux, P., Mazoyer, B., 1999. FMRI and PET of self-paced finger movement: comparison of intersubject stereotaxic averaged data. Neuroimage 10 (4), 430–447.
Jurgens, U., 1984. The efferent and afferent connections of the supplementary motor area. Brain Res. 300 (1), 63–81.
Keller, C.J., Bickel, S., Entz, L., Ulbert, I., Milham, M.P., Kelly, C., Mehta, A.D., 2011. Intrinsic functional architecture predicts electrically evoked responses in the human brain. Proc. Natl. Acad. Sci. U.S.A. 108 (25), 10308–10313.
Kochunov, P.V., Lancaster, J.L., Fox, P.T., 1999. Accurate high-speed spatial normalization using an octree method. Neuroimage 10, 724–737.
Komssi, S., Kähkönen, S., Ilmoniemi, R.J., 2004. The effect of stimulus intensity on brain responses evoked by transcranial magnetic stimulation. Hum. Brain Mapp. 21 (3), 154–164.
Koski, L., Wohlschläger, A., Bekkering, H., Woods, R.P., Dubeau, M.C., Mazziotta, J.C., Iacoboni, M., 2002. Modulation of motor and premotor activity during imitation of target-directed actions. Cereb. Cortex 12 (8), 847–855.
Kunzle, H., 1978. An autoradiographic analysis of the efferent connections from premotor and adjacent prefrontal regions (areas 6 and 9) in *Macaca fascicularis*. Brain Behav. Evol. 15, 185–234.
Lacourse, M.G., Orr, E.L., Cramer, S.C., Cohen, M.J., 2005. Brain activation during execution and motor imagery of novel and skilled sequential hand movements. Neuroimage 27 (3), 505–519.
Laird, A.R., Fox, P.M., Price, C.J., Glahn, D.C., Uecker, A.M., Lancaster, J.L., Turkeltaub, P.E., Kochunov, P., Fox, P.T., 2005. ALE meta-analysis: controlling the false discovery rate and performing statistical contrasts. Hum. Brain Mapp. 25 (1), 155–164.
Laird, A.R., Robbins, J.M., Li, K., Price, L.R., Cykowski, M.D., Narayana, S., Laird, R.W., Franklin, C., Fox, P.T., 2008. Modeling motor connectivity using TMS/PET and structural equation modeling. Neuroimage 41, 424–436.
Laird, A.R., Eickhoff, S.B., Li, K., Robin, D.A., Glahn, D.C., Fox, P.T., 2009. Investigating the functional heterogeneity of the default mode network using coordinate-based meta-analytic modeling. J. Neurosci. 29, 14496–14505.
Laird, A.R., Fox, P.M., Eickhoff, S.B., Turner, J.A., Ray, K.L., McKay, D.R., Glahn, D.C., Beckmann, C.F., Smith, S.M., Fox, P.T., 2011a. Behavioral interpretations of intrinsic connectivity networks. J. Cogn. Neurosci. 23 (12), 4022–4037.
Laird, A.R., Eickhoff, S.B., Fox, P.M., Uecker, A.M., Ray, K.L., Saenz Jr., J.J., McKay, D.R., Bzdok, D., Laird, R.W., Robinson, J.L., Turner, J.A., Turkeltaub, P.E., Lancaster, J.L., Fox, P.T., 2011b. The BrainMap strategy for standardization, sharing, and meta-analysis of neuroimaging data. BMC Res. Notes 4, 349.
Lancaster, J.L., Glass, T., Lankipalli, B.R., Downs, H., Mayberg, H., Fox, P.T., 1995. A modality-independent approach to spatial normalization of tomographic images of the human brain. Hum. Brain Mapp. 3, 209–223.
Lancaster, J.L., Fox, P.T., Downs, H., Nickerson, D.S., Hander, T.A., El Mallah, M., Kochunov, P.V., Zamarripa, F., 1999. Global spatial normalization of human brain using convex hulls. J. Nucl. Med. 40 (6), 942–955.
Lancaster, J.L., Woldorff, M.G., Parsons, L.M., Liotti, M., Freitas, C.S., Rainey, L., Kochunov, P.V., Nickerson, D., Mikiten, S.A., Fox, P.T., 2000. Automated Talairach Atlas labels for functional brain mapping. Hum. Brain Mapp. 10, 120–131.
Lancaster, J.L., Narayana, S., Wenzel, D., Luckemeyer, J., Roby, J., Fox, P.T., 2004. Evaluation of an image-guided, robotically positioned transcranial magnetic stimulation system. Hum. Brain Mapp. 22 (4), 329–340.
Lancaster, J.L., Tordesillas-Gutiérrez, D., Martinez, M., Salinas, F., Evans, A., Zilles, K., Mazziotta, J.C., Fox, P.T., 2007. Bias between MNI and Talairach coordinates analyzed using the ICBM-152 brain template. Hum. Brain Mapp. 28 (11), 1194–1205.
Lau, H.C., Rogers, R.D., Haggard, P., Passingham, R.E., 2004. Attention to intention. Science 303 (5661), 1208–1210.
Le Bihan, D., 2003. Looking into the functional architecture of the brain with diffusion MRI. Nat. Rev. Neurosci. 4 (6), 469–480.
Lehéricy, S., Ducros, M., Krainik, A., Francois, C., Van de Moortele, P.F., Ugurbil, K., Kim, D.S., 2004. 3-D diffusion tensor axonal tracking shows distinct SMA and pre-SMA projections to the human striatum. Cereb. Cortex 14 (12), 1302–1309.
Liu, Y., Gao, J.H., Liotti, M., Pu, Y., Fox, P.T., 1999. Temporal dissociation of parallel processing in the human subcortical outputs. Nature 400 (6742), 364–367.
Luppino, G., Rizzolatti, G., 2000. The organization of the frontal motor cortex. News Physiol. Sci. 15, 219–224.
Luppino, G., Matelli, M., Camarda, R., Rizzolatti, G., 1993. Corticocortical connections of area F3 (SMA-proper) and area F6 (pre-SMA) in the macaque monkey. J. Comp. Neurol. 338 (1), 114–140.
Malouin, F., Richards, C.L., Jackson, P.L., Dumas, F., Doyon, J., 2003. Brain activations during motor imagery of locomotor-related tasks: a PET study. Hum. Brain Mapp. 19 (1), 47–62.
Martin, A., 2007. The representation of object concepts in the brain. Annu. Rev. Psychol. 58, 25–45.
Matelli, M., Luppino, G., Rizzolatti, G., 1985. Patterns of cytochrome oxidase activity in the frontal agranular cortex of macaque monkey. Behav. Brain Res. 18, 125–136.
Matelli, M., Luppino, G., Rizzolatti, G., 1991. Architecture of superior and mesial area 6 and the adjacent cingulate cortex in the macaque monkey. J. Comp. Neurol. 311 (4), 445–462.
Matsumoto, R., Nair, D.R., LaPresto, E., Najm, I., Bingaman, W., Shibasaki, H., Lüders, H.O., 2004. Functional connectivity in the human language system: a cortico-cortical evoked potential study. Brain 127 (Pt 10), 2316–2330.
Matsumoto, R., Nair, D.R., LaPresto, E., Bingaman, W., Shibasaki, H., Lüders, H.O., 2007. Functional connectivity in the human cortical motor system: a cortico-cortical evoked potential study. Brain 130 (Pt 1), 181–197.
Maunsell, J.H., Van Essen, D.C., 1987. Topographic organization of the middle temporal visual area in the macaque monkey: representational biases and the relationship to

the callosal connections and myeloarchitectonic boundaries. J. Comp. Neurol. 266 (4), 535–555.
Mayka, M.A., Corcos, D.M., Leurgans, S.E., Vaillancourt, D.E., 2006. Three-dimensional locations and boundaries of motor and premotor cortices as defined by functional brain imaging: a meta-analysis. Neuroimage 31 (4), 1453–1474.
McGuire, P.K., Bates, J.F., Goldman-Rakic, P.S., 1991. Inter-hemispheric integration: I. Symmetry and convergence of the cortico-cortical connections of the left and the right principal sulcus (PS) and the left and the right supplementary motor area (SMA) in the rhesus monkey. Cereb. Cortex 1 (5), 390–407.
McKeown, M.J., Makeig, S., Brown, G.G., Jung, T.-P., Kindermann, S.S., Bell, A.J., Sejnowski, T.J., 1998. Analysis of fMRI data by blind separation into independent spatial components. Hum. Brain Mapp. 6, 160–188.
Menghini, D., Hagberg, G.E., Petrosini, L., Bozzali, M., Macaluso, E., Caltagirone, C., Vivari, S., 2008. Structural correlates of implicit learning deficits in subjects with developmental dyslexia. Ann. N. Y. Acad. Sci. 1145, 212–221.
Mori, S., Zhang, J., 2006. Principles of diffusion tensor imaging and its applications to basic neuroscience research. Neuron 51 (5), 527–539.
Narayana, S., Jacks, A., Robin, D.A., Poizner, H., Zhang, W., Franklin, C., Liotti, M., Vogel, D., Fox, P.T., 2009. A noninvasive imaging approach to understanding speech changes following deep brain stimulation in Parkinson's disease. Am. J. Speech Lang. Pathol. 18 (2), 146–161.
Ogiso, T., Kobayashi, K., Sugishita, M., 2002. The precuneus in motor imagery: a magnetoencephalographic study. Neuroreport 11 (6), 1345–1349.
Orgogozo, J.M., Larsen, B., 1979. Activation of the supplementary motor area during voluntary movement in man suggests it works as a supramotor area. Science 206, 847–850.
Passingham, R., 1993. Medial premotor area. The frontal lobes and voluntary action. Oxford University Press, Oxford.
Paus, T., Jech, R., Thompson, C.J., Comeau, R., Peters, T., Evans, A.C., 1997. Transcranial magnetic stimulation during positron emission tomography: a new method for studying connectivity of the human cerebral cortex. J. Neurosci. 17 (9), 3178–3184.
Penfield, W., Welch, K., 1951. The supplementary motor area in the cerebral cortex: a clinical and experimental study. AMA Arch. Neurol. Psychiatry 66, 289–317.
Peretz, I., Gosselin, N., Belin, P., Zatorre, R.J., Plailly, J., Tillmann, B., 2009. Music lexical networks: the cortical organization of music recognition. Ann. N. Y. Acad. Sci. 1169, 256–265.
Picard, N., Strick, P.L., 1996. Motor areas of the medial wall: a review of their location and functional activation. Cereb. Cortex 6, 342–353.
Picard, N., Strick, P.L., 2001. Imaging the premotor areas. Curr. Opin. Neurobiol. 11 (6), 663–672.
Picard, N., Strick, P.L., 2003. Activation of the supplementary motor area (SMA) during performance of visually guided movements. Cereb. Cortex 13 (9), 977–986.
Price, C.J., 2010. The anatomy of language: a review of 100 fMRI studies published in 2009. Ann. N. Y. Acad. Sci. 1191, 62–88.
Rábago, C.A., Lancaster, J.L., Narayana, S., Zhang, W., Fox, P.T., 2009. Automated-parameterization of the motor evoked potential and cortical silent period induced by transcranial magnetic stimulation. Clin. Neurophysiol. 120 (8), 1577–1587.
Rizzolatti, G., Luppino, G., Matelli, M., 1998. The organization of the cortical motor system: new concepts. Electroencephalogr. Clin. Neurophysiol. 106 (4), 283–296.
Robinson, J.L., Laird, A.R., Glahn, D.C., Lovallo, W.R., Fox, P.T., 2009. Metaanalytic connectivity modeling: delineating the functional connectivity of the human amygdala. Hum. Brain Mapp. 31 (2), 173–184.
Roland, P.E., Larsen, B., Lassen, N.A., Skinhoj, E., 1980. Supplementary motor area and other cortical areas in organization of voluntary movements in man. J. Neurophysiol. 43 (1), 118–136.
Rossini, P.M., Barker, A.T., Berardelli, A., Caramia, M.D., Caruso, G., Cracco, R.Q., et al., 1994. Non-invasive electrical and magnetic stimulation of the brain, spinal cord and roots: basic principles and procedures for routine clinical application. Report of an IFCN committee. Electroencephalogr. Clin. Neurophysiol. 91 (2), 79–92.
Sadato, N., Yonekura, Y., Waki, A., Yamada, H., Ishii, Y., 1997. Role of the supplementary motor area and the right premotor cortex in the coordination of bimanual finger movements. J. Neurosci. 17 (24), 9667–9674.
Samuel, M., Ceballos-Baumann, A.O., Blin, J., Uema, T., Boecker, H., Passingham, R.E., Brooks, D.J., 1997. Evidence for lateral premotor and parietal overactivity in Parkinson's disease during sequential and bimanual movements. A PET study. Brain. 120 (Pt 6), 963–976.
Seitz, R.J., Roland, P.E., 1992. Learning of sequential finger movements in man: a combined kinematic and positron emission tomography (PET) study. Eur. J. Neurosci. 4 (2), 154–165.
Seitz, R.J., Stephan, K.M., Binkofski, F., 2000. Control of action as mediated by the human frontal lobe. Exp. Brain Res. 133 (1), 71–80.
Smith, S.M., Fox, P.T., Miller, K.L., Glahn, D.C., Fox, P.M., Mackay, C.E., Filippini, N., Watkins, K.E., Toro, R., Laird, A.R., Beckmann, C.F., 2009. Correspondence of the brain's functional architecture during activation and rest. Proc. Natl. Acad. Sci. U.S.A. 106, 13040–13045.
Sommer, M.A., 2003. The role of the thalamus in motor control. Curr. Opin. Neurobiol. 13 (6), 663–670.
Speer, A.M., Willis, M.W., Herscovitch, P., Daube-Witherspoon, M., Shelton, J.R., Benson, B.E., Post, R.M., Wassermann, E.M., 2003a. Intensity-dependent regional cerebral blood flow during 1-Hz repetitive transcranial magnetic stimulation (rTMS) in healthy volunteers studied with H215O positron emission tomography: I. Effects of primary motor cortex rTMS. Biol. Psychiatry 54 (8), 818–825.
Speer, A.M., Willis, M.W., Herscovitch, P., Daube-Witherspoon, M., Shelton, J.R., Benson, B.E., Post, R.M., Wassermann, E.M., 2003b. Intensity-dependent regional cerebral blood flow during 1-Hz repetitive transcranial magnetic stimulation (rTMS) in healthy volunteers studied with H215O positron emission tomography: II. Effects of prefrontal cortex rTMS. Biol. Psychiatry 54 (8), 826–832.
Talairach, J., Tournoux, P., 1988. Co-planar stereotaxic atlas of the human brain: 3-dimensional proportional system: an approach to cerebral imaging. Thieme Classic.
Tanji, J., Shima, K., 1996. Supplementary motor cortex in organization of movement. Eur. Neurol. 36, 13–19.
Turkeltaub, P.E., Eden, G.F., Jones, K.M., Zeffiro, T.A., 2002. Meta-analysis of the functional neuroanatomy of single-word reading: method and validation. Neuroimage 16 (3 Pt 1), 765–780.
Van de Winckel, A., Sunaert, S., Wenderoth, N., Peeters, R., Van Hecke, P., Feys, H., Horemans, E., Marchal, G., Swinnen, S.P., Perfetti, C., De Weerdt, W., 2005. Passive somatosensory discrimination tasks in healthy volunteers: differential networks involved in familiar versus unfamiliar shape and length discrimination. Neuroimage 26 (2), 441–453.
Vogt, C., Vogt, O., 1919. Allgemeinerer Ergebnisse unserer Hirnforschung. J. Psychol. Neurol. (Leipzig) 25, 277–462.
Wiesendanger, R., Weisendanger, M., 1985b. Cerebello-cortical linkage in the monkey as revealed by transcellular labeling with the lectin wheat germ agglutinin conjugated to the marker horseradish peroxidase. Exp. Brain Res. 59 (1), 105–117.
Wiesendanger, R., Wiesendanger, M., 1985a. The thalamic connections with medial area 6 (supplementary motor cortex) in the monkey (*Macaca fascicularis*). Exp. Brain Res. 59 (1), 91–104.
Xiong, J., Parsons, L.M., Gao, J.H., Fox, P.T., 1999. Interregional connectivity to primary motor cortex revealed using MRI resting state images. Hum. Brain Mapp. 8 (2–3), 151–156.
Yarkoni, T., Poldrack, R.A., Nichols, T.E., Van Essen, D.C., Wager, T.D., 2011. Large-scale automated synthesis of human functional neuroimaging data. Nat. Methods 8 (8), 665–670.
Young, M.P., Scannell, J.W., Burns, G., 1995. The Analysis of Cortical Connectivity. Springer, Heidelberg.
Zangen, A., Roth, Y., Voller, B., Hallett, M., 2005. Transcranial magnetic stimulation of deep brain regions: evidence for efficacy of the H-coil. Clin. Neurophysiol. 116, 775–779.